A new tetra-segmented splipalmivirus with divided RdRP domains from *Cryphonectria naterciae,* a fungus found on chestnut and cork oak trees in Europe.

Yukiyo Sato[1], Sabitree Shahi[1], Paul Telengech[1], Sakae Hisano[1], Carolina Cornejo[2], Daniel Rigling[2], and Hideki Kondo[1], Nobuhiro Suzuki[1,*]

[1)]Institute of Plant Science and Resources, Okayama University, Kurashiki, 710-0046, Japan

[2)]Swiss Federal Research Institute WSL, Forest Health & Biotic Interactions, Zuercherstrasse 111, CH-8903 Birmensdorf

Running Title: New splipalmivirus from *Cryphonectria naterciae*

*Correspondence may be sent to N. Suzuki
IPSR, Okayama University
Chuou 2-20-1, Kurashiki, JAPAN
Telephone: 81-86-434-1230
FAX: 81-86-434-1232
E-mail: nsuzuki@okayama-u.ac.jp

EMBL/GenBank/DDBJ Data Library under Accession Nos. LC634419-LC634421 and LC649880

Manuscript information:
Abstract, 272 words; Text, 4,666 words excluding figures legends and references; Figures, 5; Table, 1;
Supplementary Figures, 3: Supplementary Tables, 3

Abstract

Positive-sense (+), single-stranded (ss) RNA viruses with divided RNA-dependent RNA polymerase (RdRP) domains have been reported from diverse filamentous ascomycetes since 2020. These viruses are termed splipalmiviruses or polynarnaviruses and have been characterized largely at the sequence level, but ill-defined biologically. *Cryphonectria naterciae*, from which only one virus has been reported, is an ascomycetous fungus potentially plant-pathogenic to chestnut and oak trees. We molecularly characterized multiple viruses in a single Portuguese isolate (C0614) of *C. naterciae*, taking a metatranscriptomic and conventional double-stranded RNA approach. Among them are a novel splipalmivirus (Cryphonectria naterciae splipalmivirus 1, CnSpV1) and a novel fusagravirus (Cryphonectria naterciae fusagravirus 1, CnFGV1). This study focused on the former virus. CnSpV1 has a tetra-segmented, (+)ssRNA genome (RNA1 to RNA4). As observed for other splipalmiviruses reported in 2020 and 2021, the RNA-dependent RNA polymerase domain is separately encoded by RNA1 (motifs F, A and B) and RNA2 (motifs C and D). A hypothetical protein encoded by the 5'-proximal open reading frame of RNA3 shows similarity to a counterpart conserved in some splipalmiviruses. The other RNA3-encoded protein and RNA4-encoded protein show no similarity with known proteins in a blastp search. The tetra-segment nature was confirmed by the conserved terminal sequences of the four CnSpV1 segments (RNA1 to RNA4) and their 100% coexistence in over 100 single conidial isolates tested. The experimental introduction of CnSpV1 along with CnFGV1 into a virus free strain C0754 of *C. naterciae* vegetatively incompatible with C0614 resulted in no phenotypic alteration, suggesting asymptomatic infection. The protoplast fusion assay indicates a considerably narrow host range of CnSpV1, restricted to the species *C. naterciae* and *C. carpinicola*. This study contributes to better understanding of the molecular and biological properties of this unique group of viruses.

HIGHLIGHTS

- A new splipalmivirus (CnSpV1) with divided RdRP was isolated from *C. naterciae*.
- CnSpV1 has four (+)RNA genomic segments RNA1 to RNA4.
- RNA1 and RNA2 encode divided RdRP motifs F, A and B, and C and D, respectively.
- Protoplast fusion assay suggests an extremely narrow host range of CnSpV1

1. Introduction

Fungal virus (mycovirus) studies have greatly contributed to enhanced understanding of virus diversity and evolution. Recent mycovirus hunting has revealed an array of peculiar viruses with new virus lifestyles and genome organizations in addition to viruses with some resemblance to animal and plant viruses. Examples include capsidless narna-like viruses and yadokariviruses with a positive-sense (+) single-stranded (ss) RNA genome, capsidless polymycoviruses with a multi-segmented double-stranded (ds) RNA genome. Although yadokariviruses show phylogenetic affinity to (+)ssRNA caliciviruses, they highjack the capsid protein (CP) of corresponding partner dsRNA viruses and are hypothesized to use it as the replication site, as if they were dsRNA viruses (Hisano et al., 2018; Zhang et al., 2016). Polymycoviruses are phylogenetically distantly related to caliciviruses but are infectious as deproteinized dsRNA or associated with virally encoded proline-alanine-serine rich protein (PASrp) (Jia et al., 2017; Kanhayuwa et al., 2015; Kotta-Loizou and Coutts, 2017; Sato et al., 2020a). Recently, hadakaviruses with 10- or 11-segmented (+)ssRNA genome have been discovered whose genome encodes no PASrp. The hadakavirus replicative form dsRNA is assumed to be accessible in mycelial homogenates by RNase (Khan et al., 2021; Sato et al., 2020b).

Another type of recently discovered, unusual virus is the capsidless narna-like viruses, the genomic RNA of which is expected to be associated with its RNA-dependent RNA polymerase (RdRP), the only virally encoded protein, as in the case for authentic narnaviruses (family *Narnaviridae*) (Esteban et al., 1992; Kadowaki and Halvorson, 1971; Matsumoto et al., 1990; Solorzano et al., 2000; Wickner et al., 2013). These viruses belong to the phylum *Lenarviricota* and are characterized by the smallest (+)ssRNA monopartite genome (2~5 kb) that encode only RdRP (Ayllon et al., 2020; Hillman and Cai, 2013; Wickner et al., 2013). Exceptions to this rule are plant-infecting ourmiaviruses (genus *Ourmiavirus,* family *Botourmiaviridae*) which are thought to have acquired a CP and a movement protein gene from other plant viruses most likely from a tombus-type virus (the flavi-like virus supergroup) (Rastgou et al., 2009). The RdRP is a hallmark protein that all RNA viruses (members of the kingdom *Orthornavirae* in the realm *Riboviria*) should have (Koonin et al., 2020; Walker et al., 2020; Wolf et al., 2018). All RdRPs of (+)ssRNA viruses have at least six conserved motifs F, A (DxxxxxD), B (sG---T), C (GDD), D (K/R), and E or motifs III to VIII residing on one single polypeptide (Bruenn, 2003; Koonin, 1991; Poch et al., 1989). Surprisingly, a few research groups recently discovered multiple narna-like segments with a size range of 2.1 ~ 2.5 kb by metatranscriptomic approaches which encode the aforementioned RdRP motifs in two separate segments (Chiba et al., 2021; Jia et al., 2021; Ruiz-Padilla et al., 2021; Sutela et al., 2020). These authors proposed that the multiple RNA segments represent the genome of single narna-like viruses termed splipalmiviruses (Sutela et al., 2020), polynarnaviruses (Jia et al., 2021) or binarnaviruses (Ruiz-Padilla et al., 2021). Such viral or related viral sequences were reported from diverse filamentous fungi, largely from ascomycetes,

and are increasingly growing in number. The claim that the multiple segments encoding the RdRP motifs represent a single virus and behave as an infectious entity should further be strengthened by experimental introduction with infectious nucleic acids or other infectious forms or biochemical substantiation of the replicase complex.

Cryphonectria naterciae, a filamentous ascomycete fungus, is a relatively recently established member of the genus *Cryphonectria* (order Diaporthales) that is morphologically and phylogenetically distinct from other species of the genus including *Cryphonectria parasitica* (Braganca et al., 2011). *C. naterciae* is believed to be much less pathogenic to chestnut than *C. parasitica*, a destructive pathogen of American (*Castanea dentata*) and European chestnut (*Castanea sativa*) causing blight, but it could be a secondary pathogen to weakened chestnut trees (Dennert et al., 2020). In fact, *C. naterciae* isolates were detected in European chestnut (*Castanea sativa*) trees severely affected by *C. parasitica* and cork oak (*Quercus suber*) trees with decline syndromes (Braganca et al., 2011). *C. naterciae* has not yet been extensively explored as a virus host. We searched a collection of Portuguese isolates of *C. naterciae* for mycoviruses several years ago and characterized omnipresent viruses as well as peculiar viruses such as fusagraviruses (unclassified dsRNA viruses) (Cornejo et al., 2021b).

Here we describe the molecular and biological characterization of a splipalmivirus or polynarnavirus detected in a Portuguese isolate, C0614, of *C. naterciae* co-infected with a dsRNA fusagravirus omnipresent in this fungus. This study focuses on the splipalmivirus and provides evidence of a tetra-segment nature of the splipalmivirus as the infectious unit that is highly transmissible both laterally and vertically.

2. Materials and methods

2.1 Fungal isolate, strain and growth conditions

The *C. naterciae* fungal strains, C0614 and C0754, were previously isolated from cork oak trees in Portugal by Dr. Helena Braganca at Instituto Nacional de Investigação Agrária e Veterinária (Braganca et al., 2011). The C0614 strain is a natural fungal host infecting two mycoviruses subjected to this study (a splipalmivirus and a fusagravirus). C0754 is considered to be virus-free, at least free of these two viruses, the latter of which is likely to be the most common viral agent in *C. naterciae* (Cornejo et al., 2021b). These two strains are vegetatively incompatible with each other (C. Cornejo, unpublished data). An RNA silencing deficient mutant Δ*dcl2* of *C. parasitica* was a generous gift from Dr. Donald L. Nuss at the University of Maryland (Segers et al., 2007). A European strain, DR1 (WSL collection code, M4733), of *Cryphonectria radicalis* (Hoegger et al., 2002; Shahi et al., 2021), a Japanese strain JS13 of *Cryphonectria carpinicola* (Cornejo et al., 2021a; Liu et al., 2007), a Japanese strain E16 (MAFF code, 410155) of *Cryphonectria nitchkei* and a Japanese strain AVC53 of *Valsa ceratosperma* (order Diaporthales) (Sasaki et al., 2002) were described

earlier (Hoegger et al., 2002; Shahi et al., 2021). These fungal strains were grown on Difco potato dextrose agar (PDA) or potato dextrose broth (PDB) medium (Becton, Dickinson and Co., New Jersey, USA) on the benchtop at 23–26˚C.

2.2 RNA extraction, sequencing and northern hybridization

Three-day old mycelia were used for dsRNA extraction by a method using cellulose (Advantech, Tokyo, Japan) (Eusebio-Cope and Suzuki, 2015a). The isolated dsRNA fractions were treated with DNase I (Qiagen, Hilden, Germany) and SI nuclease (Takara, Shiga, Japan) to digest genomic DNA and ssRNA, respectively, and analyzed by electrophoretic mobility on 1% agarose gel. Total RNA fractions were obtained by the method of Eusebio-Cope and Suzuki. Total RNA fractions (approximately 70 μg each) from this strain, another *C. naterciae* strain (C0613) and other five Japanese filamentous fungi were pooled evenly and sent to Macrogen Inc (Tokyo, Japan) for next-generation sequencing (NGS) (Khan et al., 2019). The five Japanese fungal strains were *C. parasitica* strains OB5-27, ES18, KZ1-31, and KZ2-39, and *C. nitschkei* strain OB4-29 (Liu et al., 2007). The cDNA library was prepared using the TruSeq RNA Sample Preparation Kit (Illumina, San Diego, CA, USA) and sequenced on the Illumina platform (HiSeq 2500, 100 bp paired-end reads) by Macrogen Inc. Qualified reads (total ~59M reads) were assembled *de novo* using CLC Genomics Workbench (version 11, CLC Bio-Qiagen). Local BLAST searches with obtained assembled fragments (26525 contigs) were performed against the viral reference sequence dataset obtained from National Center for Biotechnology Information (NCBI).

As described previously (Suzuki et al., 2004), 3'-RNA ligase mediated amplification of cDNA ends (RLM-RACE) was performed to determine the 5' and 3' terminal sequences using dsRNA as templates. The same set of oligonucleotides used as a 3RACE adaptor (5' phosphorylated oligodeoxynucleotide, 5'-PO_4-CAATACCTTCTGACCATGCAGTGACAGTCAGCATG-3'), primers for cDNA synthesis and PCR amplification were used for ligation with the 3' termini of the two dsRNAs with at 16˚C for 16–18 hrs using T4 RNA ligase (Takara Bio, Kyoto, Japan). PCR products amplified with a primer (5'-TGCATGGTCAGAAGGTATTG-3') to the ligated adaptor sequence and virus-specific primers (Table S1) were cloned into pGEM T-Easy (Promega, Madison, WI, USA) for Sanger sequencing. The splipalmivirus-RNA4 was detected by RT-PCR using primers CnSpV1-F1 (5'-CAGCATGAAACTCTTGCGAG-3') and CnSpV1-R1 (5'-GCGGCCGCTTTTTTTTTTTTTTTTTTT-3') targeting terminal sequences conserved among the other viral genomic segments. The integrity of the CnSpV1-RNA4 terminal sequence was confirmed by RLM-RACE with primers listed in Table S1. The non-viral, underlined nucleotide sequences in the primers are attached to increase melting temperature.

158 Northern blotting of ssRNA-enriched total RNA was performed according to a standard protocol
159 (Sambrook and Russell, 2001) with modification of gel composition. The modified gel was composed of
160 1% (w/v) agarose, 1×MOPS, and 1.85% (v/v) formaldehyde. Specific viral RNA bands were detected with
161 cDNA probes labeled with Digoxigenin-11-dUTP (DIG) according to the manufacture's instruction (F.
162 Hoffmann-La Roche, Ltd.). The cDNA probes labeled with Digoxigenin-11-dUTP (DIG) were prepared by
163 PCR DIG Labelling Mix (Roche, Basel, Switzerland). with primers listed in Table S1 and viral cDNA
164 templates cloned into plasmid vectors.
165
166 **2.3 Bioinformatics and phylogenetic analyses**
167 The virus genome sequences were subjected to computational analyses using GENETYX ver. 19
168 (GENETYX, Tokyo, Japan). Blast searches were run on the non-redundant (nr) DNA and protein databases
169 from NCBI (nucleotide or protein collection) (http://blast.ncbi.nlm.nih.gov/Blast.cgi).

170 Phylogenetic tree construction was carried out as described previously (Kondo et al., 2020).
171 Multiple alignments of deduced amino acid sequences were obtained by using MAFFT ver.7 (Katoh and
172 Standley, 2013). Unreliable regions of the alignments were removed using Gblocks ver. 0.91b (Talavera
173 and Castresana, 2007). The trees were then generated by the maximum-likelihood (ML) method using
174 PhyML 3.0 with model selection by Smart Model Selection (Guindon et al., 2010; Lefort et al., 2017). The
175 branch probabilities were examined by 100 bootstrap resampling. The phylogenetic trees were visualized
176 and refined using FigTree ver. 1.3.1.

177
178 **2.4 Transformation and protoplast fusion**
179 Protoplasts of a virus-free strain, C0754, *C. naterciae* were prepared by the method for *C. parasitica* as
180 described by Eusebio-Cope et al. (Eusebio-Cope and Suzuki, 2015b). The obtained protoplasts were
181 transformed with pCPXHY3 carrying a hygromycin resistant (HygR) gene (hygromycin B
182 phosphotransferase) cassette. A single conidial HygR transformant termed C0754-HygR was obtained and
183 used for protoplast fusion. As mentioned above, protoplasts were obtained from C0614 coinfected by the
184 two mycoviruses (a splipalmivirus and a fusagravirus). An equal number of protoplasts from C0614 and
185 C0754-HygR were used for protoplast fusion by using the method of Shahi et al. (Shahi et al., 2019). To
186 obtain virus-infected isolates with the C0754-HygR, regenerated protoplast fusants were selected on
187 hygromycin (Hyg)-containing solid media, potato dextrose agar-Hyg (80 μg/ml) as described by Shahi et
188 al. (Shahi et al., 2019). Regenerated fungal isolates were examined for virus infection by the colony RT-
189 PCR method (Sato et al., 2020b; Urayama et al., 2015). Primers used for RT-PCR are listed in Table S1.
190 Virus-infected hygromycin-susceptible colonies were obtained after repeated co-culturing (hyphal

anastomosis) on PDA with virus-free C0754. Similarly, the fungal strains of *C. carpinicola* JS13, *C. radicalis* DR1, *C. parasitica* Δ*dcl2*, and *V. ceratosperma* AVC5 were also tested for their ability to support the splipalmivirus infection. These fungal strains were transformed with pCPXHY3, excepting Δ*dcl2* carrying the HygR gene and JS13 transformed pCPXNeo (Andika et al., 2019), before being used as recipients.

3. Results

3.1 DsRNA profiles of strains C0614 and C0754 of *C. naterciae*

Two strains of *C. naterciae*, C0614 and C0754 were mainly used in this study. Their colony morphologies indistinguishable from each other are shown in Fig. 1A. Crude dsRNA-enrched fractions were obtained from the two strains. Their agarose gel electrophoresis patterns are shown in Fig. 1B. A dsRNA band of approximately 10-kbp was detectable from strain C0614, whereas no dsRNA band was observed in C0754. The 10-kbp band represents the genomic dsRNA of a novel fusagravirus termed Cryphonectria naterciae fusagravirus 1 (CnFGV1) and its details will soon be published (Cornejo et al., 2021b).

3.2 Sequence analysis and genome organization of a novel splipalmivirus

The NGS data of a pooled sample of *C. naterciae* C0613 and C0614, and five Japanese strains of *Cryphonectria spp.* revealed two narna-like contigs, ctg1325 and ctg700, and other virus-like contigs derived from three fusagravirus strains, Cryphonectria hypovirus 1 (CHV1, a hypovirus), Cryphonectria nitschkei chrysovirus 1 (CnCV1, an alphachrysovirus) and Cryphonectria parasitica bipartite mycovirus 1 (a dsRNA virus). See Table S3 for detailed local-blast analysis of the NGS data. The novel narna-like virus, the main subject of this study, was designated as Cryphonectria naterciae splipalmivirus 1 (CnSpV1) which shows sequence similarities with members of a newly proposed group, "Splipalmivirus". CnSpV1 was detected by RT-PCR only from C0614, but not from the other *Cryphonectria* strains. "Splipalmivirus" was named after their divided (split) nature of the RdRP palm subdomains (Sutela et al., 2020) that is the most essential and composed of motifs A to D (Smertina et al., 2019). For this group of viruses, other name candidates, polynarnavirus and binarnavirus have been proposed. Because multi-segmented narna-like viruses with the undivided RdRP domains have been reported (Charon et al., 2019; Jia et al., 2021; Shi et al., 2016), we have adopted "splipalmivirus" reflecting this group properly. The ctg1325 and ctg700 each harbored single open reading frames (ORFs) that hypothetically encoded N- and C-terminal parts of the RdRP, respectively, as divided forms (Fig. 2A). The protein encoded by ctg1325 (CnSpV1-P1) contained RdRP motif F, A, and B (Fig. S1), while that encoded by ctg700 (CnSpV1-P2) had RdRP motif C and D (Fig. S2). CnSpV1 probably utilizes the nuclear genetic code, not the mitochondrial one, like narnaviruses and unlike mitovirids. The known splipalmiviruses are supposed to have bi-, tri-, quad, or septuple-

segmented genomes (Chiba et al., 2021; Jia et al., 2021; Ruiz-Padilla et al., 2021; Sutela et al., 2020). We compared global amino acid sequence identity among some of those splipalmiviruses divided RdRPs and narnaviruses RdRPs (Fig. 2B). CnSpV1-P1 and -P2 showed higher identity to the counterparts of Aspergillus fumigatus narnavirus 2 (AfuNV2) (Chiba et al., 2021) (44.8% and 41.0%, respectively) than the other tested proteins (Fig. 2B). Using the splipalmiviral genomes that were available from GenBank in Apr 2021 as a reference, we found an additional splipalmi-like contig, ctg1142, from the NGS data of strain C0614 (data not shown). The ctg1142 showed weak homology to a hypothetical protein that was encoded by RNA3 of the three isolates of AfuNV2 (36.4–37.1% identity under 28% query coverage by BLASTX). After terminal sequencing by RACE, we named the full-length CnSpV1 genomic RNA segments corresponding to ctg1325, ctg700, and ctg1142 as CnSpV1-RNA1, -RNA2, and -RNA3, respectively (Fig. 2A). To investigate whether CnSpV1 had additional genomic segments, we performed RT-PCR with primers targeting the 5'- and 3'-terminal sequences strictly conserved regions among three RNA segments. This analysis revealed a new segment termed RNA4 that was also found from NGS data as ctg2558 (data not shown). RNA4 only possessed a small ORF with no significant sequence similarity to known sequences (Fig. 2A). The four RNA segments shared the 13 nucleotides at the 5'-terminus, while they had a poly (A) tail at the 3'-terminus (Fig. 2C). Well-conserved sequence stretches were observed preceding the poly (A) tail across four CnSpV1 genomic segments (Fig. 2C).

CnSpV1-RNA3 encodes two non-overlapping ORFs that are designated ORF3-1 and ORF3-2 (Fig. 2A and S3A). The hypothetical protein encoded by ORF3-1 showed homology only to a hypothetical protein encoded by AfuNV2-RNA3, while that encoded by ORF3-2 showed no homology to any protein by blastp search of the database non-redundant protein sequences (nr) (using algorithm "blastp" with default settings). ORF3-2 is situated at -2 or +1 frame relative to ORF3-1. There is no typical slippery sequence (Atkins et al., 2016) that allows for -2 or +1 ribosomal frameshifting at the ORF junction region (Fig. S3B). If the -2 or +1 frameshift occurs at the site, a fusion protein from the ORF3-1 and ORF3-2 would be generated (Fig. S3A). However, it is unknown how the second ORF (ORF3-2) is expressed and we cannot rule out the possibility of other non-cannonical expression strategy. Domain database search (Marchler-Bauer et al., 2017) revealed that the N-terminal part of the potential fusion protein contained a conserved domain termed RPP1A (COG2058) (Fig. S3A) found in some eukaryotic ribosomal proteins. RNA3 and RNA4 of splipalmiviruses are mono- or poly-cistronic (Fig. S3C). Like CnSpV1-RNA3, AfuNV2-RNA3 has bi- or tri-cistronic ORFs (Chiba et al., 2021). Unlike the case of CnSpV1-RNA3, however, the latter ORFs of AfuNV2 are located at +0 and -1 frame relative to the former ORF (Fig. S3C). Only the protein encoded by the first ORF of each CnSpV1-RNA3 and AfuNV2-RNA3 showed a relatively higher global identity (Fig. S3D), which is consistent with the above-mentioned blast result. The sequence conservation of the first ORF implies that the protein encoded by that might play some conserved biological role.

Because an RNA pool from several fungal strains, i.e., *C. naterciae* strain C0614 and several Japanese fungal strains was used for next-generation sequencing analysis (see Materials and Methods), we confirmed that the four segments were from one particular strain. The four segments, i.e., RNA1, RNA2, RNA3, and RNA4, were present in the original fungal strain C0614, but not from the virus-free strain C0754, by northern blotting (Fig. 2D).

3.3 Phylogenetic analyses of CnSpV1

The phylogenetic relationships of CnSpV1 with other splipalmiviruses and narna-like viruses were analyzed based on the deduced amino acid sequence of proteins P1 with the RdRP_A and _B motifs and P2 with the RdRP_C and _D motifs together with corresponding RdRP regions of monopartite narna-like viruses. In both ML trees, the known splipalmiviruses and their candidates form three well-supported clades highlighted light pink, blue and yellow (Fig. 3). These viruses are distantly related to two monopartite narna-like virus groups (named as sub-clades 1 and 2) and more distantly related to authentic narnaviruses represented by Saccharomyces 20S narnavirus (Fig. 3). CnSpV1 falls within one splipalmivirus clade together with other splipalmivirus candidates previously isolated from *Aspergillus* and phytopathogenic fungi.

3.3 Efficient vertical and horizontal transmission of CnSpV1

First, we obtained sub-isolates via single conidial isolation from the original *C. naterciae* C0614 coinfected with CnSpV1 and CnFGV1 for two purposes: 1) to identify the infection unit of CnSpV1 and 2) to obtain virus-free sub-isolates for investigating the effect of CnSpV1 on *C. natercia*. We tested over 100 sub-isolates for the presence of RNA1 to RNA4 using specific primer sets for each of the four RNA sequences. One-step colony RT-PCR results showed that all of the tested isolates provided a PCR product of the expected size for RNA1, RNA2, RNA3, or RNA4 (Table S1), while no amplification was detected in the negative control strain, C0754, with any of the CnSpV1 primer sets (Fig. 4). In addition, a CnFGV1-specific fragment of 600 bp was detected in all of the obtained single conidial sub-isolates. Neither virus-free sub-isolates nor single infectants were observed after screening over 100 sub-isolates (Fig. 4, data not shown). These indicate the coinfection of all the sub-isolates by both CnSpV1 and CnFGV1. Importantly, all the four RNA segments of CnSpV1 were transmitted to each sub-isolate, strongly suggesting that the four RNA segments represent the infectious entity of CnSpV1, which is highly transmissible vertically. However, we could not achieve objective 2, investigation of the possible effect of CnSpV1 on the host.

Next, we performed protoplast fusion between C0614 and a virus-free strain, hygromycin-resistant C0754-HygR, of *C. naterciae*, granted that CnSpV1 could be laterally transmitted between the two strains

of the same species. C0754-HygR was prepared by transforming C0754-derived protoplasts by pCPXHY3. The primary screening was carried out on PDA-Hyg post protoplast fusion (see step 3 of Fig. 1 of Shahi et al. (Shahi et al., 2019)). All 20 sub-isolates selected on PDA-HygR likely possessed the C0754-HygR genetic background and harbored both CnSpV1 and CnFGV1 (Table 1). Of these isolates four were co-cultured with the original hygromycin-susceptible C0754 strain repeatedly (see step 4 of Fig. 1 of Shahi et al. (Shahi et al., 2019)). All tested recipient strains with the C0754 genetic background were found to be stably infected by the two viruses (Fig. 5A). These results indicate that CnSpV1 can infect another strain of *C. naterciae*, and can be efficiently transmitted horizontally via hyphal fusion in *C. naterciae*. Stable co-transmission of the four genomic segments of CnSpV1 via the hyphal fusion was observed. C0754-HygR infected by CnSpV1 and CnFGV1 after the repeated hyphal fusion showed indistinguishable colony morphology and growth to virus-free C0754-HygR (Fig. 5B).

3.4 An extremely narrow host range of, and possible asymptomatic infection by CnSpV1

Our failure to separately isolate the two coinfecting viruses prompted us to test other fungi as their hosts in the expectation that they differentially infect them. To this end, five other fungal strains were used as recipients: *C. parasitica* Δ*dcl2*, *C. radicalis* DR1, *C. carpinicola* JS13, *C. nitschkei* E16 and *V. ceratosperma* AVC53. At least a total of 20 isolates were examined at the primary screening step for CnSpV1 presence in each assay. However, no CnSpV1-positive isolates were obtained, in contrast to the intra-species protoplast fusion between strains C0614 (donor) and C0754HygR (recipient) which provided 100% infection of primarily selected isolates of the recipient isolates (Table 1). This was the case for protoplast fusion assays between C0614 (donor) and *V. ceratosperma* AVC53 (recipient), *C. radicalis* DR1 (recipient), or *C. parasitica* Δ*dcl2* (recipient) lacking the primary antiviral defense. Note that all isolates, in most cases, derived from protoplast fusion with the tested four strains as recipients were CnFGV1-positive (Table 1), and that CnFGV1 infection was maintained in the recipient genetic background even after repeated co-culturing (Fig. 5C). These results indicate that protoplast fusion occurred and CnFGV1 could be transferred to the recipient fungal strains. *C. carpinicola* JS13 (recipient) was different from the above four strains and was found to receive CnSpV1 only infrequently via protoplast fusion (Table 1). The genetic background of the CnSpV1-positive single-conidial isolate was confirmed by vegetative compatibility with original virus-free JS13. Once acquired by JS13, CnSpV1 was readily transferred to virus-free JS13.

Taken together, these results suggest that CnSpV1 has a very narrow host range, restricted to the species *C. naterciae*, and cannot infect other species even within the genus *Cryphonectria*.

4. Discussion

The RNA-dependent RNA polymerase gene is the hallmark for the members of the kingdom *Orthornavirae* within the realm *Riboviria,* regardless of whether their genomes are (+)ssRNA, (-)ssRNA or dsRNA. RdRPs generally have at least six motifs A through F and are encoded by single genes (Bruenn, 2003; Koonin, 1991; Poch et al., 1989). It is noteworthy that RdRPs in a different order of motifs C→A→B in place of A→B→C, were reported in a few RNA viruses with dsRNA or (+)ssRNA genomes, but reside on single polypeptides (Gorbalenya et al., 2002; Sabanadzovic et al., 2009). Motifs A to D comprise the most conserved "palm" subdomain of the right-hand-like structure of RdRP, which is responsible for RNA polymerization. Motifs E and F make up the "thumb" and "finger" subdomains, respectively (Smertina et al., 2019). In this sense, splipalmiviruses recently discovered from fungi are unique exceptions. All reported splipalmiviruses including the newly characterized CnSpV1 appear to be variable in genome segment number from 2 to 7, but commonly encode motifs F, A, and B on RNA1, while motifs C and D are encoded by RNA2. This split motif profile is conserved in all reported splipalmiviruses.

Splipalmiviruses are phylogenetically related to members of the phylum *Lenarviricota* accommodating four families *Leviviridae*, *Mitoviridae*, *Narnaviridae* and *Botourmiaviridae*. Levivirids are bacterial phages exemplified by *Escherichia* virus Qbeta, while mitoviruses are mitochondrially replicated either in fungal or some plant hosts (Hillman and Cai, 2013; Nerva et al., 2019; Nibert et al., 2018). Members of the other two families are considered to replicated cytosolically in fungal or plant hosts with a capsidless nature and lack mitochondrial codon usage, i.e., UGA for tryptophan. Splipalmiviruses remain officially unassigned, but are most closely related to monopartite narna-like viruses exemplified by Plasmopara viticola associated narnavirus 11 (Chiapello et al., 2020) and likely are classified into a new class or family within the phylum *Lenarviricota* (Sutela et al., 2020). Interestingly the two trees based on RNA1- and RNA2-encoded divided RdRP proteins showed a similar topology (Fig. 3). Reported splipalmiviruses were grouped into three clades for which three genera "Unuasplipalmivirus", "Duasplipalmivirus" and "Triasplipalmivirus" are proposed within the family "Splipalmiviridae" (Fig. 3). CnSpV1 is most closely related to an *Aspergillus* virus (AfuNV2) among the splipalmi-related viruses whose divided RdRP-encoding genomic segments have been revealed (Fig. 2B and Fig. 3). AfuNV2 appears to have three genomic segments homologous to RNA1 to RNA3 of CnSpV1, though its tri-segmented genome nature unproven biologically.

Genome segmentation of RNA viruses during the course of evolution are occasionally documented. Examples include monopartite potyviruses and bipartite bymoviruses within the family *Potyviridae*, monopartite closteroviruses and bipartite criniviruses within the family *Closteroviridae*, and many monopartite rhabdovirids and bipartite dichorhaviruses with the family *Rhabdoviridae* (Fuchs et al., 2020; Walker et al., 2018; Wylie et al., 2017). Splipalmiviruses are fundamentally different from these viruses in two aspects. Firstly, no division of the RdRP motifs was observed in such viruses. Therefore, it is of great

interest to investigate whether the two proteins encoded by RNA1 and RNA2 make up the RdRP complex with the palm domain similar to regular undivided viral RdRPs. Secondly, no unsegmented form of splipalmiviruses (family "Splipalmiviridae") has yet been detected. That is, no viruses have been found with an undivided genome with the coding capacity for P1and P2 or all together with other proteins such as P3. Capsidless narna- and narna-like viruses and fungal botourmiaviruses are the simplest form of RNA viruses that encode only RdRPs, and are predicted to have been derived from bacterial phage levivirus after losing a few genes such as capsid protein genes. Reverse genetics tools demonstrated that the RdRP-encoding segments are sufficient for virus viability in narnaviruses and related eukaryote-infecting viruses of the phylum *Lenarviricota* (Esteban and Fujimura, 2003; Esteban et al., 2005; Retallack et al., 2021; Wang et al., 2020). To investigate the possible biological significance of the multisegment nature of these viruses will be a future challenge. Further investigation of the functional roles of each segment in virus replication should be possible after establishment of reverse genetics tools.

Little is known about the biology of splipalmiviruses, i.e., their infectivity, symptomatology, and transmissibility. In this study, taking advantage of a protoplast fusion protocol (Honda et al., 2020; Shahi et al., 2021; Shahi et al., 2019) and single spore isolation, we showed that the four segments of the novel splipalmivirus CnSpV1 behave as an infectious unit and likely causes asymptomatic infection in *C. naterciae* (Fig. 5). All of the four segments were transmitted through conidia and fused recipients in an all-or-none fashion (Figs. 4 and 5), in which no loss of segments was observed unlike multisegmented fungal viruses (Sato et al., 2018). A bi-segment nature was also confirmed for a splipalmivirus, Botrytis cinerea binarnavirus 2 via single spore isolation (Ruiz-Padilla et al., 2021). Our observation suggests that all the segments are essential for the completion of infection cycle. In this study, we could not obtain a virus -free strain from C0614 despite repeated attempts. Thus, we transferred CnSpV1 to the virus-free strain C0754 of *C. naterciae* by protoplast fusion. The observation that two isogenic strains, the original C0754 and CnSpV1-carrying C0754 were indistinguishable in phenotype (Fig. 5) suggest that CnSpV1 causes symptomless infection on a growth media. However, CnSpV1-carrying C0754 also harbored CnFGV1, which necessitates further investigation to draw a decisive conclusion.

There are only a limited number of fungal viruses whose host ranges have been thoroughly investigated. The prototype hypovirus CHV1 can be replicated in *V. ceratosperma*, as well as one strain of Phomopsis G-type (teleomorph *Diaporthe* Nitschke) (Sasaki et al., 2002), both being members of the family Valsaceae different from Cryphonectriae accommodating *C. parasitica*. Several members of the genus *Cryphonectria* and related genus *Endothia* were shown to host CHV1 (Chen et al., 1996). The replication of a mitochondrially replicating mitovirus, Cryphonectria parasitica mitovirus 1 can be supported only by some members of the genera *Cryphonectria* and *Valsa* (Shahi et al., 2019). The host range of a dsRNA chrysovirus CnCV1 is limited to a few members of the genus *Cryphonectria,* and the virus cannot replicate

in *C. parasitica* (Shahi et al., 2021). A fusarivirus, Fusarium graminearum virus DK21 was shown to be able to replicate in *Fusarium* spp. as well as in *C. parasitica* (Lee et al., 2011). Relative to the above viruses, the host range of CnSpV1 is much narrower and limited to the different strain of the same species, *C. naterciae* and *C. carpinicola*. Other species within the genus *Cryphonectria* did not allow for CnSpV1 replication. This conclusion was strengthened by the protoplast fusion results in which the co-infecting CnFGV1 was transferred to *Cryphonectria* spp. and *V. ceratosperma* non-host to CnSpV1 (Table 1). These observations suggest the intimate interactions between CnSpV1 and host factors specifically present in *C. naterciae* and *C. carpinicola.* Of note is that *C. naterciae* is phylogenetically closer to *C. carpinicola* than to *C. parasitica* or *C. nitschkei* (Cornejo et al., 2021a).

Virus replication and transmission in general are governed by many factors. Among them is antiviral RNA silencing which has a negative impact on virus replication, as well as horizontal and vertical transmission (Chiba and Suzuki, 2015; Sun et al., 2006; Suzuki et al., 2003). It should be noted that a fungal reovirus, mycoreovirus 2 (MyRV2), of *C. parasitica* cannot be stably maintained likely due to antiviral RNA silencing (Aulia et al., 2019; Aulia et al., 2021). Only when RNA silencing is deficient or compromised, MyRV2 can be stably maintained in its host fungus. The inability of CnSpV1 to replicate in *Cryphonectria* spp. other than *C. naterciae* is due unlikely to antiviral RNA silencing. This assumption is based on the observation that even in the *C. parasitica* Δ*dcl2,* CnSpV1 was unable to replicate (Table 1 or Fig. 5). Rather, as aforementioned, CnSpV1 replication necessitates some factors specifically present in *C. naterciae* but absent in other *Cryphonectiria* spp.

This study clearly demonstrated high vertical (Fig. 4) and lateral (Fig. 5) transmission rates of CnSpV1 in the original host *C. naterciae*. We failed to obtain virus-free fungal isolates or isolates singly infected by CnSpV1 from the original strain C0614 doubly infected by CnSpV1 and CnFGV1. However, CnFGV1 could be replicated in other species of the genus *Cryphonectria*, indicating its full-fledged nature. There are different types of interactions between coinfecting viruses as reported for other virus combinations (Hillman et al., 2018; Sasaki et al., 2016). The co-presence of CnSpV1 and CnFGV1 leads to the speculation that CnSpV1 relies on CnFGV1 in some way in its replication cycle. Although we cannot conclude on the intimate interplay between CnSpV1 and CnFGV1, it may be unlikely because of many infections by splipalmiviruses without fusagraviruses.

Acknowledgments

This study was supported in part by Yomogi Inc., Joint Usage/Research Center, Institute of Plant Science and Resources, Okayama University (to CC), the Ohara Foundation for Agriculture Research (to NS), Grants-in-Aid for Scientific Research (A) and Grants-in-Aid for Scientific Research on Innovative Areas

and Grants-in-Aid for JSPS fellows from the Japanese Ministry of Education, Culture, Sports, Science and Technology (KAKENHI 21H05035, 21K18222, 17H01463, 16H06436, 16H06429 and 16K21723 to N.S and H.K.; 19J00261 to YS). The authors are grateful to Drs. Donald L. Nuss, for generous gifts of the *C. parasitica* strain Δ*dcl2*. YS and SS are JSPS (Japan Society for the Promotion of Science) fellows.

Compliance with ethical standards

Conflict of interest

The authors declare that they have no conflict.

Ethical approval

This article does not contain any studies with human participants or animals performed by any of the authors.

Figure legends

Fig. 1 Colony morphologies and dsRNA patterns of *Cryphonectria naterciae* strains C0614 and C0754. (A) Colony morphology of *Cryphonectria naterciae* strains C0614 and C0754. The fungal colonies were grown on PDA for six days and photographed. (B) Agarose gel electrophoresis of dsRNA fractions from strains C0614 and C0754. A crude dsRNA fraction containing host fungal ribosomal RNA (rRNA) obtained from fungal mycelia was electrophoresed on a 1% agarose gel. M-dsDNA shows the molecular size of dsDNA with GeneRuler 1 kb DNA ladder (Thermo Fischer Scientific, Inc., Massachusetts, U.S.A.).

Fig. 2. Genome organization of CnSpV1. (A) Genome map of Cryphonectria naterciae splipalmivirus 1 (CnSpV1). The solid lines indicate positive-sense single-stranded genomic RNA. The colored boxes indicate hypothetical open reading frames (ORFs). The light-blue bars above the genomic segments show the position of DIG-labelled probes (Fig. 2D) and RT-PCR fragments (Figs. 4 and 5). The GenBank accession numbers assigned to the CnSpV1 genomic segments are LC634419 (RNA1), LC634420 (RNA2), LC634421 (RNA3) and LC649880 (RNA4). **(B)** Pairwise percent identity matrix of RdRPs of splipalmiviruses and narnaviruses. Full names of viruses and accession numbers of their proteins are listed in Table S2. Left and right panels show the comparison among the divided RdRP of splipalmiviruses [splipalmi-P1 (containing F/A/B motif) or -P2 (containing C/D motif), respectively] with undivided RdRP of narnaviruses (narna-P1). The identity is based on a global multiple sequence alignment by Clustal Omega version 1.2.4 (Sievers et al., 2011). The heatmap was drawn by R package "gplots" version 3.1.1. **(C)** Comparison of nucleotide terminal sequences among CnSpV1 genomic RNA segments. The full-length

457 RNA segments were subjected to the alignment by MUSCLE (Edgar, 2004) in GENETYX-MAC Network
458 version 20.1.0. Sequence heterogeneity, detected at certain positions among RACE clones, is shown by the
459 letters D (A, G or T), B (G, T or C), or W (A or T). **(D)** Northern blotting of the CnSpV1 genomic RNAs.
460 SsRNA-enriched total RNA (5 μg per lane) fractions were obtained from two *C. naterciae* isolates, C0614
461 and virus-free C0754. M-ssRNA refers to ssRNA size standards [ssRNA Ladder (New England Biolabs,
462 Inc, Massachusetts, U.S.A.)].

463 **Fig. 3 Phylogeny of the RdRP of splipalmiviruses and narnaviruses.** The maximum likelihood (ML)
464 trees were constructed using PhyML 3.0 based on the multiple amino acid sequence alignments of
465 splipalmivirus-P1 with the RdRP_A and B motifs (**A**) or splipalmivirus-P2 with the RdRP_C and D motifs
466 (**B**), and the corresponding RdRP regions of monopartite narna-like viruses. The LG + I + G and LG + G
467 were selected as best-fitting substitution models for the splipalmivirus-P1 and splipalmivirus-P2,
468 respectively. GenBank accession numbers of viruses are followed by their virus names. A set of
469 splipalmivirus-like sequences in the *Puccinia triticina* transcriptomic data (no. GISY01077803 and
470 GIKZ01037126) was also included in this analysis. The putative phylogroups of splipalmiviruses are shown
471 with different colored boxes. The two phylogroups for monopartite narna-like viruses, tentatively named
472 sub-clades 1 and 2, are displayed as collapsed triangles. Their members are listed in the right-side box. Two
473 narnaviruses, Saccharomyces 23S RNA narnavirus and Saccharomyces 20S RNA narnavirus were used as
474 the outgroups. Three genera, "Unuasplipalmivirus", "Duasplipalmivirus", and "Triasplipalmivirus" and
475 one family "Splipalmiviridae" have been proposed to accommodate splipalmiviruses. The scale bar
476 represents amino acid distances. The numbers at the nodes are bootstrap values of >50% in 100 iterations.

477

478 **Fig. 4. Simultaneous detection of RNA1 to RNA4 of CnSpV1 in single conidial isolates.**

479 Single conidial sub-isolates were obtained from the original CnSpV1-infected strain C0641 and examined
480 for the virus presence by one-step colony RT-PCR (see Materials and Methods). RT-PCR was set to detect
481 five different RNA targets: CnSpV1 RNA1, RNA2, RNA3, and RNA4 and CnFGV1. Amplified fragments
482 were electrophoresed on a 1.2% agarose gel in a 1 x TBE buffer system. The sequences of primers used are
483 shown in Table S1. Positions of the RT-PCR amplicons of CnSpV1 are illustrated in Fig. 2A. M refers to
484 DNA size standards [GeneRuler 1 kb DNA ladder (Thermo Fisher Scientific, Inc.)].

485

486 **Fig. 5 Horizontal transfer of CnSpV1 in *C. naterciae* and *C. parasitica*.**

(**A**) Colony RT-PCR was performed to detect CnSpV1 and CnFGV1 in C0754-derived fungal recipient isolates after coculturing with strain C0754-Hyg co-infected with CnSpV1 and CnFGV1. Primer sets used in this panel and panel (C) for detection of CnSpV1 and CnFGV1 are shown in Table S1. (**B**) Colony growth and morphology were compared between virus-free and -infected strain C0754. The fungal strains were grown on PDA for four days and photographed and subjected to area measurements by ImageJ. The means and standard deviations were calculated from three sub-isolates. (**C**) RT-PCR products with the CnSpV1 RNA1- (top panel) or CnFGV1-specific primer sets (bottom) were electrophoresed as in Fig. 4.

Supplementary figure legends

Fig. S1. Multiple alignment of amino acid sequences of spliparmivirus-P1 (N-terminal part of the divided RdRP) and narnavirus-P1 (undivided RdRP). Amino acid sequences were aligned by MAFFT online version 7.475 with L-INS-i method (Katoh et al., 2019). Part of the alignment is shown. Full names of the viruses and accession numbers are listed in Table S2. Analyzed viruses are the same as Fig. 2B and Fig. S2.

Fig. S2. Multiple alignment of amino acid sequences of spliparmivirus-P2 (C-terminal part of the divided RdRP) and narnavirus-P1 (undivided RdRP). Amino acid sequences were aligned as described in the legend to Fig. S1. Part of the alignment is shown. Full names of the viruses and accession numbers are listed in Table S2. Analyzed viruses are the same as Fig. 2B and Fig. S1.

Fig. S3. Hypothetical proteins encoded by CnSpV1-RNA3. (A) Hypothetical frameshift products encoded by CnSpV1-RNA3. The schematic diagram for the putative -2 and +1 frameshift products from CnSpV1-RNA3 was shown below its genome map. The hypothetical frameshift products contained RPP1A (ribosomal protein L12E/L44/L45/RPP1/RPP2, COG2058) domain at the amino acid positions 18-97 with an e-value $4.71e^{-3}$. The conserved domain was predicted by DELTA-BLAST search of non-redundant protein sequences (nr) provided by NCBI. **(B)** The nucleotide sequence around the intergenic region of the two hypothetical ORFs on CnSpV1-RNA3. The sequence was visualized in GENETIX-MAC version 20.1.0. **(C)** Schematic representation of the splipalmiviruses non-RdRP-encoding segments. **(D)** Pairwise percent identity matrix of the non-RdRP-proteins of splipalmiviruses. Viruses full names and accession numbers of the proteins are listed in Table S2. The analysis was performed as described in the legend for Fig. 2B. The left panel shows the comparison between the CnSpV1-P3-1 and AfuNV2-P3 with MoNV1

proteins. The right panel shows the comparison between CnSpV1-P3-2 and AfuNV2-P5 with MoNV1 proteins.

References

Andika, I.B., Kondo, H., Suzuki, N., 2019. Dicer functions transcriptionally and post-transcriptionally in a multilayer antiviral defense. Proc Natl Acad Sci U S A 116, 2274-2281. doi/2210.1073/pnas.1812407116

Atkins, J.F., Loughran, G., Bhatt, P.R., Firth, A.E., Baranov, P.V., 2016. Ribosomal frameshifting and transcriptional slippage: From genetic steganography and cryptography to adventitious use. Nucleic Acids Research 44(15), 7007-7078.

Aulia, A., Andika, I.B., Kondo, H., Hillman, B.I., Suzuki, N., 2019. A symptomless hypovirus, CHV4, facilitates stable infection of the chestnut blight fungus by a coinfecting reovirus likely through suppression of antiviral RNA silencing. Virology 533, 99-107.

Aulia, A., Hyodo, K., Hisano, S., Kondo, H., Hillman, B.I., Suzuki, N., 2021. Identification of an RNA Silencing Suppressor Encoded by a Symptomless Fungal Hypovirus, Cryphonectria Hypovirus 4. Biology (Basel) 10(2), 100 doi:110.3390/biology10020100.

Ayllon, M.A., Turina, M., Xie, J., Nerva, L., Marzano, S.L., Donaire, L., Jiang, D., Consortium, I.R., 2020. ICTV Virus Taxonomy Profile: Botourmiaviridae. J Gen Virol 101(5), 454-455.

Braganca, H., Rigling, D., Diogo, E., Capelo, J., Phillips, A., Tenreiro, R., 2011. *Cryphonectria naterciae*: a new species in the *Cryphonectria-Endothia* complex and diagnostic molecular markers based on microsatellite-primed PCR. Fungal Biol 115(9), 852-861.

Bruenn, J.A., 2003. A structural and primary sequence comparison of the viral RNA-dependent RNA polymerases. Nucleic Acids Res 31(7), 1821-1829.

Charon, J., Grigg, M.J., Eden, J.S., Piera, K.A., Rana, H., William, T., Rose, K., Davenport, M.P., Anstey, N.M., Holmes, E.C., 2019. Novel RNA viruses associated with Plasmodium vivax in human malaria and Leucocytozoon parasites in avian disease. PLoS Pathog 15(12), e1008216. doi: 1008210.1001371/journal.ppat.1008216.

Chen, B.S., Chen, C.H., Bowman, B.H., Nuss, D.L., 1996. Phenotypic changes associated with wild-type and mutant hypovirus RNA transfection of plant pathogenic fungi phylogenetically related to Cryphonectria parasitica. Phytopathology 86, 301-310.

Chiapello, M., Rodriguez-Romero, J., Ayllon, M.A., Turina, M., 2020. Analysis of the virome associated to grapevine downy mildew lesions reveals new mycovirus lineages. Virus Evol 6(2), veaa058 doi: 010.1093/ve/veaa1058.

Chiba, S., Suzuki, N., 2015. Highly activated RNA silencing via strong induction of dicer by one virus can interfere with the replication of an unrelated virus. Proc Natl Acad Sci U S A 112(35), E4911-E4918.

Chiba, Y., Oiki, S., Yaguchi, T., Urayama, S.I., Hagiwara, D., 2021. Discovery of divided RdRp sequences and a hitherto unknown genomic complexity in fungal viruses. Virus Evol 7(1), veaa101 doi: 110.1093/ve/veaa1101.

Cornejo, C., Hauser, A., Beenken, L., Cech, T., Rigling, D., 2021a. *Cryphonectria carpinicola* sp. nov. associated with hornbeam decline in Europe. Fungal Biol 125(5), 347-356. doi: 310.1016/j.funbio.2020.1011.1012.

Cornejo, C., Hisano, S., Bragança, H., Suzuki, N., Rigling, D., 2021b. A new double-stranded mycovirus in *Cryphonectria naterciae* able to cross the species barrier and deleterious to new host. Journal of Fungi (in press).

Dennert, F., Rigling, D., Meyer, J.B., Schefer, C., Augustiny, E., Prospero, S., 2020. Testing the pathogenic potential of *Cryphonectria parasitica* and related species on three common European Fagaceae. Frontiers in Forests and Global Change 3.

Edgar, R.C., 2004. MUSCLE: multiple sequence alignment with high accuracy and high throughput. Nucleic Acids Res 32(5), 1792-1797.

Esteban, L.M., Rodriguezcousino, N., Esteban, R., 1992. T double-stranded RNA (dsRNA) sequence reveals that T and W-dsRNAs form a new RNA family in *Saccharomyces cerevisiae* . Identification of 23 S RNA as the single-stranded Form of T dsRNA. J Biol Chem 267(15), 10874-10881.

Esteban, R., Fujimura, T., 2003. Launching the yeast 23S RNA Narnavirus shows 5' and 3' cis-acting signals for replication. Proc Natl Acad Sci U S A 100, 2568-2573.

Esteban, R., Vega, L., Fujimura, T., 2005. Launching of the yeast 20S RNA narnavirus by expressing the genomic or antigenomic viral RNA in vivo. J Biol Chem 280, 33725-33734.

Eusebio-Cope, A., Suzuki, N., 2015a. Mycoreovirus genome rearrangements associated with RNA silencing deficiency. Nucleic Acids Res 43(7), 3802-3813.

Eusebio-Cope, A., Suzuki, N., 2015b. Mycoreovirus genome rearrangements associated with RNA silencing deficiency. Nucleic Acids Res 43(7), 3802-3813.

Fuchs, M., Bar-Joseph, M., Candresse, T., Maree, H.J., Martelli, G.P., Melzer, M.J., Menzel, W., Minafra, A., Sabanadzovic, S., Report Consortium, I., 2020. ICTV virus taxonomy profile: *Closteroviridae*. J Gen Virol 101(4), 364-365.

Gorbalenya, A.E., Pringle, F.M., Zeddam, J.L., Luke, B.T., Cameron, C.E., Kalmakoff, J., Hanzlik, T.N., Gordon, K.H.J., Ward, V.K., 2002. The palm subdomain-based active site is internally permuted in viral RNA-dependent RNA polymerases of an ancient lineage. J Mol Biol 324(1), 47-62.

Guindon, S., Dufayard, J.F., Lefort, V., Anisimova, M., Hordijk, W., Gascuel, O., 2010. New algorithms and methods to estimate maximum-likelihood phylogenies: assessing the performance of PhyML 3.0. Syst Biol 59(3), 307-321.

Hillman, B.I., Aulia, A., Suzuki, N., 2018. Viruses of plant-interacting fungi. Adv Virus Res 100, 99-116.

Hillman, B.I., Cai, G., 2013. The family *Narnaviridae*: simplest of RNA viruses. Adv Virus Res 86, 149-176.

Hisano, S., Zhang, R., Faruk, M.I., Kondo, H., Suzuki, N., 2018. A neo-virus lifestyle exhibited by a (+)ssRNA virus hosted in an unrelated dsRNA virus: Taxonomic and evolutionary considerations. Virus Res 244, 75-83.

Hoegger, P.J., Rigling, D., Holdenrieder, O., Heiniger, U., 2002. *Cryphonectria radicalis*: rediscovery of a lost fungus. Mycologia 94(1), 105-115.

Honda, S., Eusebio-Cope, A., Miyashita, S., Yokoyama, A., Aulia, A., Shahi, S., Kondo, H., Suzuki, N., 2020. Establishment of Neurospora crassa as a model organism for fungal virology. Nat Commun 11, 5627 DOI: 5610.1038/s41467-41020-19355-y.

Jia, H., Dong, K., Zhou, L., Wang, G., Hong, N., Jiang, D., Xu, W., 2017. A dsRNA virus with filamentous viral particles. Nat Commun 8(1), 168.

Jia, J., Fu, Y., Jiang, D., Mu, F., Cheng, J., Lin, Y., Li, B., Marzano, S.L., Xie, J., 2021. Interannual dynamics, diversity and evolution of the virome in Sclerotinia sclerotiorum from a single crop field. Virus Evol 7(1), veab032 doi: 010.1093/ve/veab1032.

Kadowaki, K., Halvorson, H.O., 1971. Appearance of a new species of ribonucleic acid during sporulation in *Saccharomyces cerevisiae*. J Bacteriol 105(3), 826-830.

Kanhayuwa, L., Kotta-Loizou, I., Ozkan, S., Gunning, A.P., Coutts, R.H., 2015. A novel mycovirus from *Aspergillus fumigatus* contains four unique dsRNAs as its genome and is infectious as dsRNA. Proc Natl Acad Sci U S A 112(29), 9100-9105.

609 Katoh, K., Rozewicki, J., Yamada, K.D., 2019. MAFFT online service: multiple sequence alignment,
610 interactive sequence choice and visualization. Brief Bioinform 20(4), 1160-1166.
611 Katoh, K., Standley, D.M., 2013. MAFFT multiple sequence alignment software version 7: improvements
612 in performance and usability. Mol Biol Evol 30(4), 772-780.
613 Khan, H.A., Sato, Y., Kondo, H., Jamal, A., Bhatti, M.F., Suzuki, N., 2021. A second capsidless hadakavirus
614 strain with 10 positive-sense single-stranded RNA genomic segments from Fusarium nygamai.
615 Arch Virol 166, 2711-2722.
616 Kondo, H., Fujita, M., Hisano, H., Hyodo, K., Andika, I.B., Suzuki, N., 2020. Virome analysis of aphid
617 populations that Infest the barley field: the discovery of two novel groups of nege/kita-like
618 viruses and other novel RNA viruses. Front Microbiol 11, ARTN 509. doi:
619 510.3389/fmicb.2020.00509.
620 Koonin, E.V., 1991. The phylogeny of RNA-dependent RNA polymerases of positive-strand RNA viruses. J
621 Gen Virol 72 (Pt 9), 2197-2206.
622 Koonin, E.V., Dolja, V.V., Krupovic, M., Varsani, A., Wolf, Y.I., Yutin, N., Zerbini, F.M., Kuhn, J.H., 2020.
623 Global organization and proposed megataxonomy of the virus world. Microbiol Mol Biol Rev
624 84(2), e00061-00019.
625 Kotta-Loizou, I., Coutts, R.H.A., 2017. Studies on the virome of the entomopathogenic fungus *Beauveria*
626 *bassiana* reveal novel dsRNA elements and mild hypervirulence. Plos Pathogens 13(1),
627 e1006183.
628 Lee, K.M., Yu, J., Son, M., Lee, Y.W., Kim, K.H., 2011. Transmission of Fusarium boothii mycovirus via
629 protoplast fusion causes hypovirulence in other phytopathogenic fungi. PLoS One 6(6), e21629.
630 Lefort, V., Longueville, J.E., Gascuel, O., 2017. SMS: Smart Model Selection in PhyML. Mol Biol Evol 34(9),
631 2422-2424.
632 Liu, Y.C., Dynek, J.N., Hillman, B.I., Milgroom, M.G., 2007. Diversity of viruses in *Cryphonectria parasitica*
633 and *C. nitschkei* in Japan and China, and partial characterization of a new chrysovirus species.
634 Mycol Res 111, 433-442.
635 Marchler-Bauer, A., Bo, Y., Han, L., He, J., Lanczycki, C.J., Lu, S., Chitsaz, F., Derbyshire, M.K., Geer, R.C.,
636 Gonzales, N.R., Gwadz, M., Hurwitz, D.I., Lu, F., Marchler, G.H., Song, J.S., Thanki, N., Wang, Z.,
637 Yamashita, R.A., Zhang, D., Zheng, C., Geer, L.Y., Bryant, S.H., 2017. CDD/SPARCLE: functional
638 classification of proteins via subfamily domain architectures. Nucleic Acids Res 45(D1), D200-
639 D203.
640 Matsumoto, Y., Fishel, R., Wickner, R.B., 1990. Circular single-stranded RNA replicon in *Saccharomyces*
641 *cerevisiae*. Proc Natl Acad Sci U S A 87(19), 7628-7632.
642 Nerva, L., Vigani, G., Di Silvestre, D., Ciuffo, M., Forgia, M., Chitarra, W., Turina, M., 2019. Biological and
643 molecular characterization of Chenopodium quinoa mitovirus 1 reveals a distinct small RNA
644 response compared to those of cytoplasmic RNA viruses. J Virol 93(7), e01998-01918.
645 Nibert, M.L., Vong, M., Fugate, K.K., Debat, H.J., 2018. Evidence for contemporary plant mitoviruses.
646 Virology 518, 14-24.
647 Poch, O., Sauvaget, I., Delarue, M., Tordo, N., 1989. Identification of four conserved motifs among the
648 RNA-dependent polymerase encoding elements. EMBO J 8(12), 3867-3874.
649 Rastgou, M., Habibi, M.K., Izadpanah, K., Masenga, V., Milne, R.G., Wolf, Y.I., Koonin, E.V., Turina, M.,
650 2009. Molecular characterization of the plant virus genus Ourmiavirus and evidence of inter-
651 kingdom reassortment of viral genome segments as its possible route of origin. J Gen Virol 90(Pt
652 10), 2525-2535.
653 Retallack, H., Popova, K.D., Laurie, M.T., Sunshine, S., DeRisi, J.L., 2021. Persistence of ambigrammatic
654 narnaviruses requires translation of the reverse open reading frame. J Virol, 10.1128/JVI.00109-
655 00121.

Ruiz-Padilla, A., Rodriguez-Romero, J., Gomez-Cid, I., Pacifico, D., Ayllon, M.A., 2021. Novel mycoviruses discovered in the mycovirome of a necrotrophic fungus. mBio 12(3), e03705-03720. doi: 03710.01128/mBio.03705-03720.

Sabanadzovic, S., Ghanem-Sabanadzovic, N.A., Gorbalenya, A.E., 2009. Permutation of the active site of putative RNA-dependent RNA polymerase in a newly identified species of plant alpha-like virus. Virology 394(1), 1-7.

Sambrook, J., Russell, D.W., 2001. Molecular cloning: a laboratory manual, 3rd edn. Cold Spring Harbor Laboratory, Cold Spring Harbor, N.Y.

Sasaki, A., Nakamura, H., Suzuki, N., Kanematsu, S., 2016. Characterization of a new megabirnavirus that confers hypovirulence with the aid of a co-infecting partitivirus to the host fungus, *Rosellinia necatrix*. Virus Res 219, 73-82.

Sasaki, A., Onoue, M., Kanematsu, S., Suzaki, K., Miyanishi, M., Suzuki, N., Nuss, D.L., Yoshida, K., 2002. Extending chestnut blight hypovirus host range within diaporthales by biolistic delivery of viral cDNA. Mol Plant Microbe Interact 15, 780-789.

Sato, Y., Caston, J.R., Suzuki, N., 2018. The biological attributes, genome architecture and packaging of diverse multi-component fungal viruses. Curr Opin Virol 33, 55-65.

Sato, Y., Jamal, A., Kondo, H., Suzuki, N., 2020a. Molecular characterization of a novel polymycovirus from *Penicillium janthinellum* with a focus on its genome-associated PASrp. Front Microbiol 11, 592789.

Sato, Y., Shamsi, W., Jamal, A., Bhatti, M.F., Kondo, H., Suzuki, N., 2020b. Hadaka virus 1: a capsidless eleven-segmented positive-sense single-stranded RNA virus from a phytopathogenic fungus, *Fusarium oxysporum*. mBio 11(3), e00450-00420. DOI: 00410.01128/mBio.00450-00420.

Segers, G.C., Zhang, X., Deng, F., Sun, Q., Nuss, D.L., 2007. Evidence that RNA silencing functions as an antiviral defense mechanism in fungi. Proc Natl Acad Sci U S A 104, 12902-12906.

Shahi, S., Chiba, S., Kondo, H., Suzuki, N., 2021. Cryphonectria nitschkei chrysovirus 1 with unique molecular features and a very narrow host range. Virology 554, 55-65.

Shahi, S., Eusebio-Cope, A., Kondo, H., Hillman, B.I., Suzuki, N., 2019. Investigation of host range of and host defense against a mitochondrially replicating mitovirus. J Virol 93(6), e01503-01518.

Shi, M., Lin, X.D., Tian, J.H., Chen, L.J., Chen, X., Li, C.X., Qin, X.C., Li, J., Cao, J.P., Eden, J.S., Buchmann, J., Wang, W., Xu, J., Holmes, E.C., Zhang, Y.Z., 2016. Redefining the invertebrate RNA virosphere. Nature 540(7634), 539-543.

Sievers, F., Wilm, A., Dineen, D., Gibson, T.J., Karplus, K., Li, W., Lopez, R., McWilliam, H., Remmert, M., Soding, J., Thompson, J.D., Higgins, D.G., 2011. Fast, scalable generation of high-quality protein multiple sequence alignments using Clustal Omega. Mol Syst Biol 7, 539.

Smertina, E., Urakova, N., Strive, T., Frese, M., 2019. Calicivirus RNA-dependent RNA polymerases: Evolution, structure, protein dynamics, and function. Front Microbiol 10, 1280.

Solorzano, A., Rodriguez-Cousino, N., Esteban, R., Fujimura, T., 2000. Persistent yeast single-stranded RNA viruses exist in vivo as genomic RNA center dot RNA polymerase complexes in 1 : 1 stoichiometry. J Biol Chem 275(34), 26428-26435.

Sun, L., Nuss, D.L., Suzuki, N., 2006. Synergism between a mycoreovirus and a hypovirus mediated by the papain-like protease p29 of the prototypic hypovirus CHV1-EP713. J Gen Virol 87, 3703-3714.

Sutela, S., Forgia, M., Vainio, E.J., Chiapello, M., Daghino, S., Vallino, M., Martino, E., Girlanda, M., Perotto, S., Turina, M., 2020. The virome from a collection of endomycorrhizal fungi reveals new viral taxa with unprecedented genome organization. Virus Evol 6(2), veaa076.

Suzuki, N., Maruyama, K., Moriyama, M., Nuss, D.L., 2003. Hypovirus papain-like protease p29 functions in trans to enhance viral double-stranded RNA accumulation and vertical transmission. J Virol 77, 11697-11707.

Suzuki, N., Supyani, S., Maruyama, K., Hillman, B.I., 2004. Complete genome sequence of Mycoreovirus-1/Cp9B21, a member of a novel genus within the family *Reoviridae*, isolated from the chestnut blight fungus *Cryphonectria parasitica*. J Gen Virol 85, 3437-3448.

Talavera, G., Castresana, J., 2007. Improvement of phylogenies after removing divergent and ambiguously aligned blocks from protein sequence alignments. Syst Biol 56(4), 564-577.

Urayama, S., Katoh, Y., Fukuhara, T., Arie, T., Moriyama, H., Teraoka, T., 2015. Rapid detection of Magnaporthe oryzae chrysovirus 1-A from fungal colonies on agar plates and lesions of rice blast. J Gen Plant Pathol 81(2), 97-102.

Walker, P.J., Blasdell, K.R., Calisher, C.H., Dietzgen, R.G., Kondo, H., Kurath, G., Longdon, B., Stone, D.M., Tesh, R.B., Tordo, N., Vasilakis, N., Whitfield, A.E., Ictv Report, C., 2018. ICTV Virus Taxonomy Profile: *Rhabdoviridae*. J Gen Virol 99(4), 447-448.

Walker, P.J., Siddell, S.G., Lefkowitz, E.J., Mushegian, A.R., Adriaenssens, E.M., Dempsey, D.M., Dutilh, B.E., Harrach, B., Harrison, R.L., Hendrickson, R.C., Junglen, S., Knowles, N.J., Kropinski, A.M., Krupovic, M., Kuhn, J.H., Nibert, M., Orton, R.J., Rubino, L., Sabanadzovic, S., Simmonds, P., Smith, D.B., Varsani, A., Zerbini, F.M., Davison, A.J., 2020. Changes to virus taxonomy and the statutes ratified by the International Committee on Taxonomy of Viruses (2020). Arch Virol 165(11), 2737-2748.

Wang, Q.H., Mu, F., Xie, J.T., Cheng, J.S., Fu, Y.P., Jiang, D.H., 2020. A single ssRNA segment encoding RdRp Is sufficient for replication, infection, and transmission of ourmia-like virus in fungi. Front Microbiol 11, 379.

Wickner, R.B., Fujimura, T., Esteban, R., 2013. Viruses and prions of *Saccharomyces cerevisiae*. Adv Virus Res 86, 1-36.

Wolf, Y.I., Kazlauskas, D., Iranzo, J., Lucia-Sanz, A., Kuhn, J.H., Krupovic, M., Dolja, V.V., Koonin, E.V., 2018. Origins and evolution of the global RNA virome. mBio 9(6), e02329-02318 doi: 02310.01128/mBio.02329-02318.

Wylie, S.J., Adams, M., Chalam, C., Kreuze, J., Lopez-Moya, J.J., Ohshima, K., Praveen, S., Rabenstein, F., Stenger, D., Wang, A., Zerbini, F.M., Ictv Report, C., 2017. ICTV Virus Taxonomy Profile: *Potyviridae*. J Gen Virol 98(3), 352-354.

Zhang, R., Hisano, S., Tani, A., Kondo, H., Kanematsu, S., Suzuki, N., 2016. A capsidless ssRNA virus hosted by an unrelated dsRNA virus. Nat Microbiol 1, 15001 doi:15010.11038/NMICROBIOL.12015.15001.

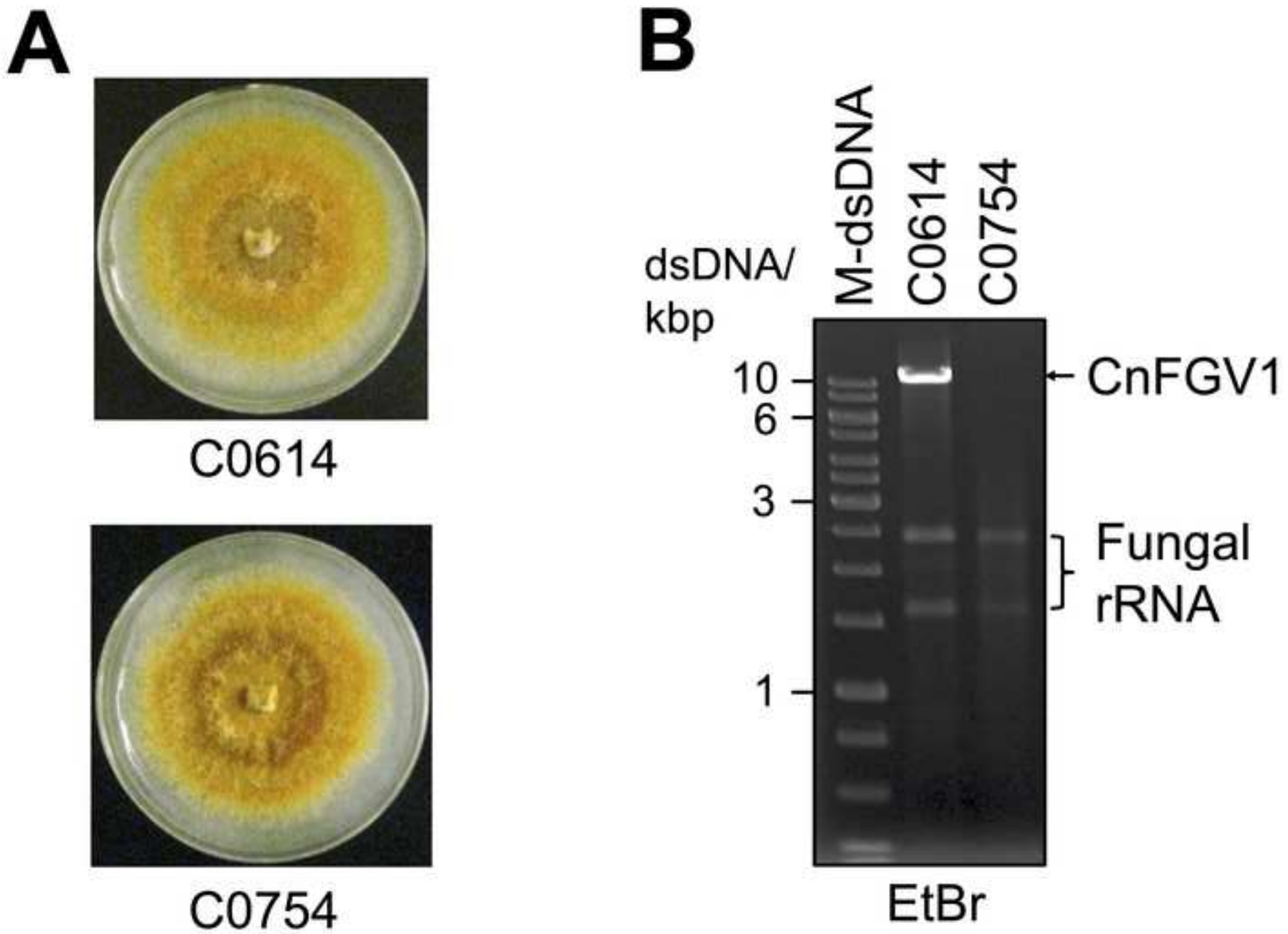

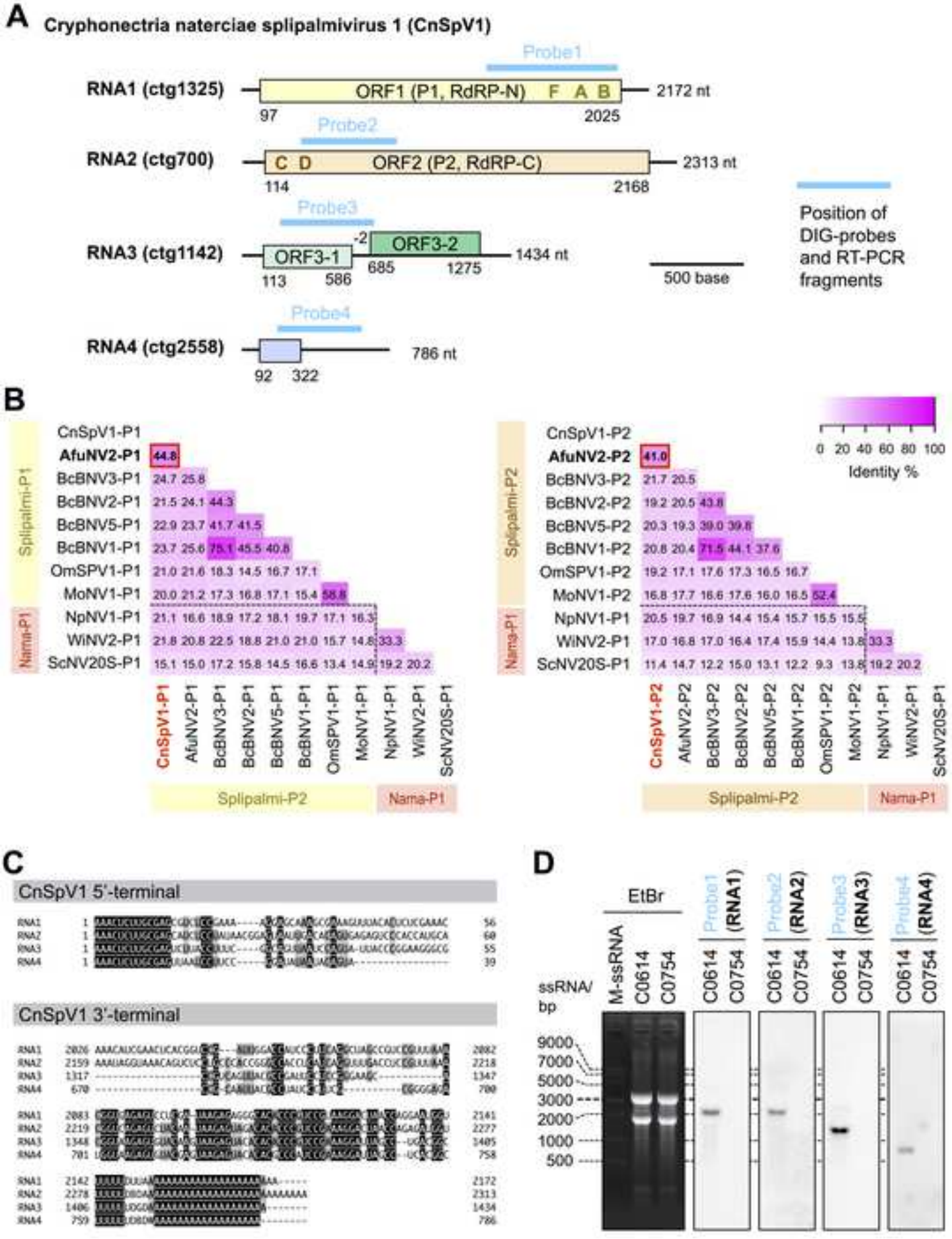

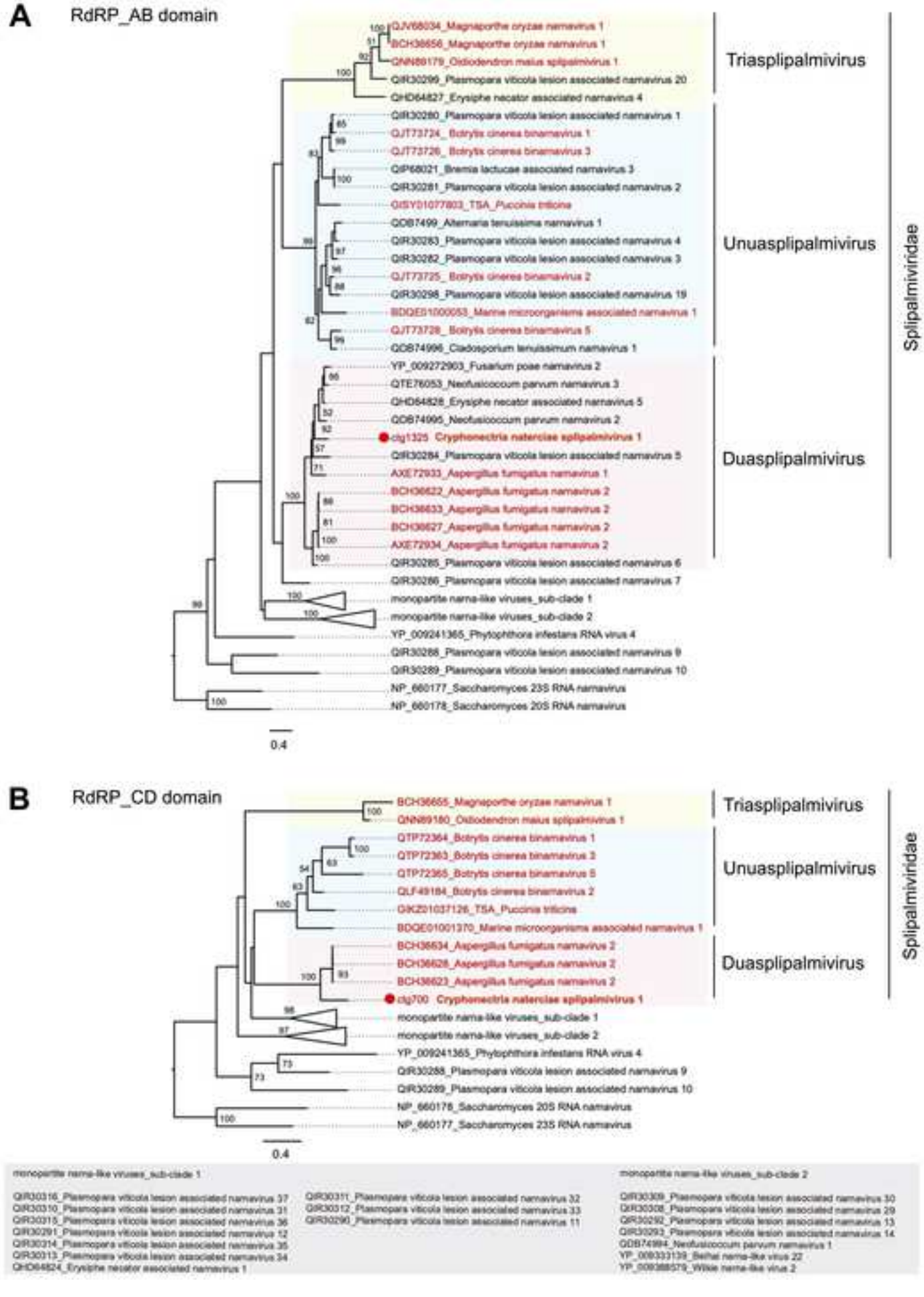

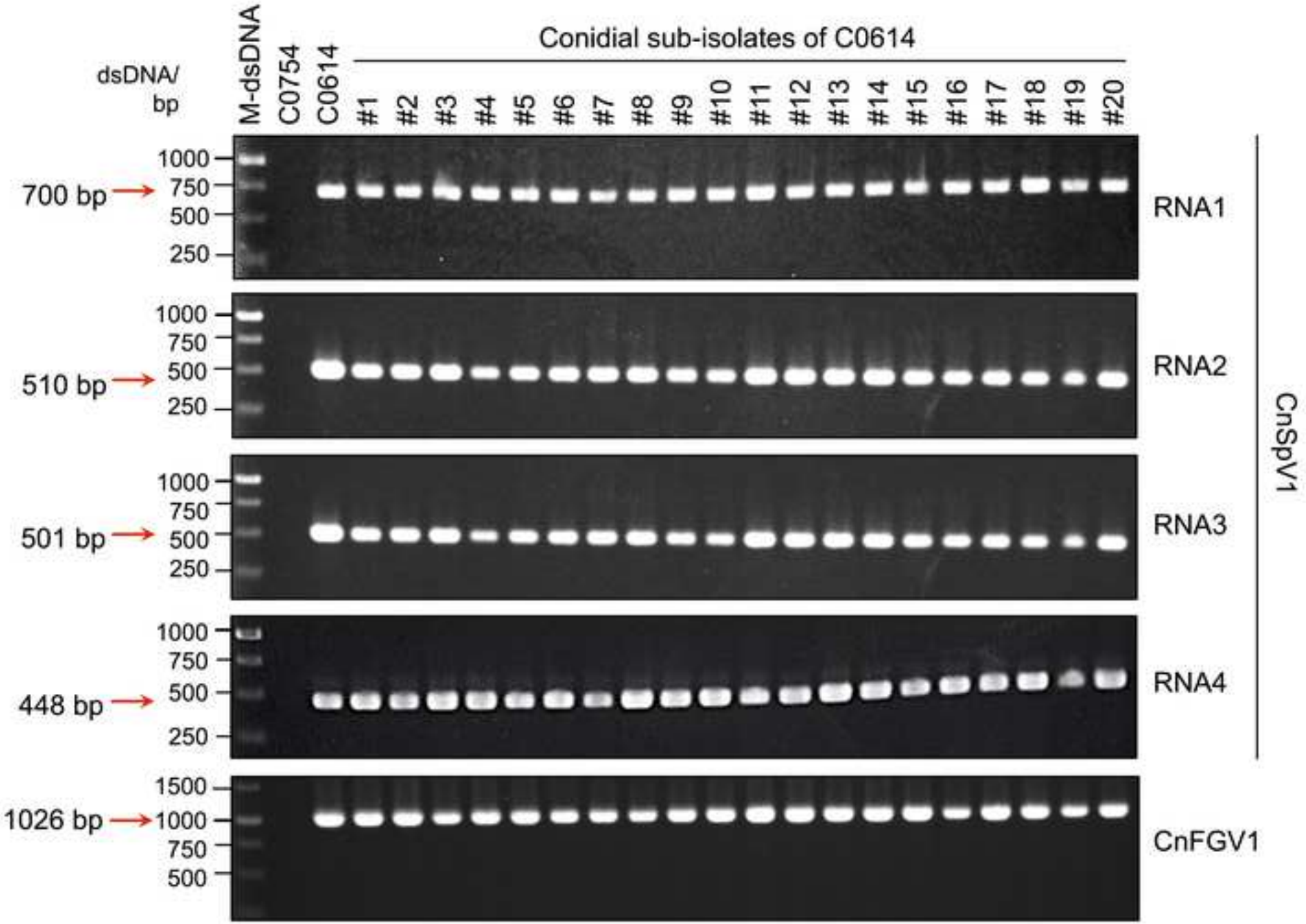

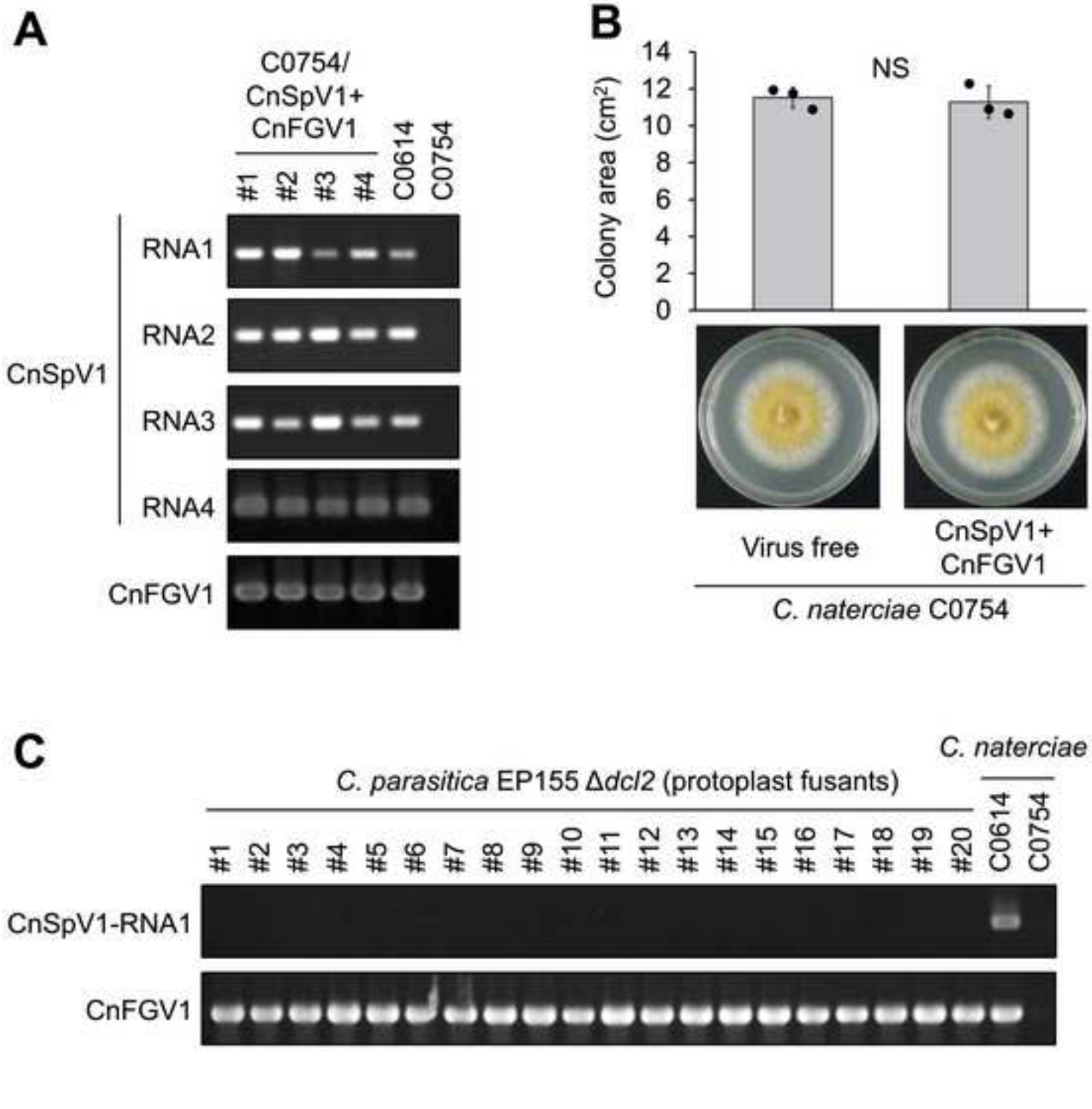

736 **Table 1. Horizontal transfer of CnSpV1 via protoplast fusion**

737

738

Fungal species	Fungal strain (Recipients)	Donor strain: *C. naterciae* C0614 carrying CnSpV1 +CnFGV1			
		Experiment I (detection rate*)		Experiment II (detection rate)	
		CnSpV1	CnFGV1	CnSpV1	CnFGV1
Cryphonectria naterciae	C0754-HygR	**20/20 (100%)**	**20/20 (100%)**	**20/20 (100%)**	**20/20 (100%)**
C. parasitica	Δ*dcl2*	**0/20 (0%)**	**20/20 (100%)**	**0/20 (0%)**	**20/20 (100%)**
C. radicalis	DR1	**0/20 (0%)**	**20/20 (100%)**	**0/20 (0%)**	**20/20 (100%)**
C. carpinicola	JS13	**0/20 (0%)**	**20/20 (100%)**	**1/20 (5%)**	**20/20 (100%)**
C. nitschkei	E16	**0/20 (0%)**	**3/20 (15%)**	**0/20 (0%)**	**1/20 (5%)**
Valsa ceratosperma	AVC53	**0/20 (0%)**	**20/20 (100%)**	**0/20 (0%)**	**19/20 (95%)**

739 *tested by direct colony one-step RT-PCR

740

741

Supplementary Data for

A new tetra-segmented splipalmivirus with divided RdRP domains from *Cryphonectria naterciae,* a fungus found on chestnut and cork oak trees in Europe.

Yukiyo Sato[1], Sabitree Shahi[1], Paul Telengech[1], Sakae, Hisano[1], Carolina Cornejo[2], Daniel Rigling[2], and Hideki Kondo[1], Nobuhiro Suzuki[1,*]

[1)]Institute of Plant Science and Resources, Okayama University, Kurashiki, 710-0046, Japan

[2)]Swiss Federal Research Institute WSL, Forest Health & Biotic Interactions, Zuercherstrasse 111, CH-8903 Birmensdorf

Running Title: New splipalmivirus from *Cryphonectria naterciae*

*Correspondence may be sent to N. Suzuki
IPSR, Okayama University
Chuou 2-20-1, Kurashiki, JAPAN
TEL: 81-86-434-1230
FAX: 81-86-434-1232
E-mail: nsuzuki@okayama-u.ac.jp

EMBL/GenBank/DDBJ Data Library under Accession Nos. LC634419-LC634421 and LC649880

Supplementary Figures, 3: Supplementary Tables, 3

Supplementary figure legends

Fig. S1. Multiple alignment of amino acid sequences of spliparmivirus-P1 (N-terminal part of the divided RdRP) and narnavirus-P1 (undivided RdRP). Amino acid sequences were aligned by MAFFT online version 7.475 with L-INS-i method (Katoh et al., 2019). Part of the alignment is shown. Full names of the viruses and accession numbers are listed in Table S2. Analyzed viruses are the same as Fig. 2B and Fig. S2.

Fig. S2. Multiple alignment of amino acid sequences of spliparmivirus-P2 (C-terminal part of the divided RdRP) and narnavirus-P1 (undivided RdRP). Amino acid sequences were aligned as described in the legend to Fig. S1. Part of the alignment is shown. Full names of the viruses and accession numbers are listed in Table S2. Analyzed viruses are the same as Fig. 2B and Fig. S1.

Fig. S3. Hypothetical proteins encoded by CnSpV1-RNA3. (A) Hypothetical frameshift products encoded by CnSpV1-RNA3. The schematic diagram for the putative -2 and +1 frameshift products from CnSpV1-RNA3 was shown below its genome map. The hypothetical frameshift products contained RPP1A (ribosomal protein L12E/L44/L45/RPP1/RPP2, COG2058) domain at the amino acid positions 18-97 with an e-value $4.71e^{-3}$. The conserved domain was predicted by DELTA-BLAST search of non-redundant protein sequences (nr) provided by NCBI. **(B)** The nucleotide sequence around the intergenic region of the two hypothetical ORFs on CnSpV1-RNA3. The sequence was visualized in GENETIX-MAC version 20.1.0. **(C)** Schematic representation of the splipalmiviruses non-RdRP-encoding segments. **(D)** Pairwise percent identity matrix of the non-RdRP-proteins of splipalmiviruses. Viruses full names and accession numbers of the proteins are listed in Table S2. The analysis was performed as described in the legend for Fig. 2B. The left panel shows comparison between the CnSpV1-P3-1 and AfuNV2-P3 with MoNV1 proteins. The right panel shows the comparison between CnSpV1-P3-2 and AfuNV2-P5 with MoNV1 proteins.

FIG S1


Motif F
Splipalmi-P1
CnSpV1-P1 --------SVYERNVMSVRVSLVAELGKFRAITVSHLAHAVLLHVLSHVLLKYL-SAVPS
AfuNV2-P1 --------NIYSSNSMSCRISLVAELGKYRTITVSSLQHALLLHPMSHIGLKIL-EVIPS
BcBNV1-P1 ----------PEDLKRAFVTVVKEPGKGRTVTKASAALKIVLDLVSRLCAEPLKKGIAS
BcBNV3-P1 ----------PEDLKRAFVTVVKEPGKGRTVTKASAALKIVLDFVSRLCAEPMKKGIAS
BcBNV2-P1 ----------RDALKMAFLTVVKEPGKARSVTKARACLKVVLDLVNKICSEPLKKGIKS
BcBNV5-P1 ----------PEELRKVYLTVVREPSKARVVTKGHAALKIVLDTISKICSWPLKKGFAS
OmSPV1-P1 -HLFMVNGEPYRPPVMDAQIVHISEPGKERNLTKSHAVLAWFLTPASKITQGTL-AHLPE
MoNV1-P1 YHRFPTQVGEYQPDIMNAKIVHISEPGKERNLTKSHATYAWFLTPGAKLSQAIL-AVLPE
Narna-P1
NpNV1-P1 ----------PTYVRCVRVHSVVEPSKARTITVAPYAYQVIMGVLAHMYQATL--QHKH
WiNV2-P1 ----------RQKVTEVTLSVVNEPSKARTITVGDYALVQLLNVAAHIFKDVC--CTQP
ScNV20S-P1 ----------NGSDPKGRVSVVRERGHKVRVVSAMETHELVL----------
Motif A
Splipalmi-P1
CnSpV1-P1 SESGVKAANHAWNFFKRLSHKNPSANFIFG----------DKDVYLFSTD
AfuNV2-P1 SQSGIGAANHAWNFFKRLSHKNPSASFIFK----------EDIESSVLSTD
BcBNV1-P1 SQSGMGKSHHGWNFFLSLMTLEKREELF---AVEKRDQREFAEYIERLDIYADLFVSSTD
BcBNV3-P1 SRSGMGKSHHGWNFFLSLMSLENKEDLF---RVAQRDEREFADYVERLDIYADLFVSSTD
BcBNV2-P1 SASGMGASNHGWNLFVSMMTEEERADVF---DLHSREENAYEGYVERTDTFSDLFVASTD
BcBNV5-P1 SASGMGKSHHGWNLFKDMTS-EEMADLMFCEDRARRVEDAFNDHIDRTQYWQDLWFSSTD
OmSPV1-P1 HRAGLLESGHEWRHQKRISALSDESGFIYDPSTGK----------TRWEVRQVFKD
MoNV1-P1 HRAGLLESGHEWRHQKRISPLSDESGFVYDSRTGK----------VYPEIRHVFKD
Narna-P1
NpNV1-P1 VKSGLKADRHLWRFVQKVLNPQSAEWQHLP----------EGATIYALSTD
WiNV2-P1 VRSGMRADRHLFNFVWKDLHPQNTLWDDMGWSYET----------KGMPIHALSSD
ScNV20S-P1 ---GHAARRRLFKGLRRERRLRDTLKGDFEATTKAF----------VGCAGTVISSD
Motif A
Splipalmi-P1
CnSpV1-P1 WEQATDYCNQMTAQAILNNLCQV------LGIPGYYRQTCVFALCAPRQIEEI-------
AfuNV2-P1 WESATDYCDPYIAGAMLNRLLYR------LGVPQWYRETVLFALTAPRQVETL-------
BcBNV1-P1 YRTATDYLHHDVAREAGDGWMRK------CGIPPILRGIVNMSCYTGRDIYFMGTGPLAQ
BcBNV3-P1 YKTATDYLHHDVARELGDAWMRK------CGIPDILRGIVCMTCYTPRNIYFTGTGPLAK
BcBNV2-P1 YEEATDRLPHKMGSDLAGMWMRK------CGIPPLLRGIVQETCFKPRRVFFYATGVLET
BcBNV5-P1 FQEATDRLVHSIAQPIGSAWMKK------CGIPPLLQGIVIGTCFQPRTVYFTATGPLKH
OmSPV1-P1 WTESTDFICKAVGWAHLKALLDY------IGFPSMYGRLVLKTIVEPQPVVEVTHRI---
MoNV1-P1 WTESTDFISKSVGYVHLRTFFDY------VAFPAAYGRLILKTIVEPQPVVEVVSHV---
Narna-P1
NpNV1-P1 LSEATDFGNLTVSRQIWQFLIKLSSV--HEGFPTGLAVLGKTLYNGARFFFV--------
WiNV2-P1 LETATDYANPSVGRQIWDCLISGLEIQYPESSPRALLELCRDLHVGPRTVYY--------
ScNV20S-P1 MKSASDLIPLSVASAIVDGLEAS-----GRLLPVEIAGL--RACTGPQHLVYP-------
Motif B
Splipalmi-P1
CnSpV1-P1 -----SQENKTL-ERY----FTTRGELMGDPVTKVILHYYHLVARESAVMA---------
AfuNV2-P1 -----DRNGCPI-EVF----YTSRGVLMGDPVTKVVLHLHHLIGAKIAGLL---------
BcBNV1-P1 IGEAANDLGQNV-RKV----RLVRGVLMGDPLTKVVLHMINILSRTIGVEM---------
BcBNV3-P1 YGENADEFGQNI-RRI----RLVRGVLMGDPLTKVVLHMVNICTRTIGVNM---------
BcBNV2-P1 IGTAEPTMGIGV-RSV----PLLKGVLMGDPLTKVVLHLTNVITRHLGTRM---------
BcBNV5-P1 IGL--PTGGEDE-NKI----TLRRGVLMGDPLTKVVLHLVNIIIRDLGQGM---------
OmSPV1-P1 ----QVEGGEDIVEPVEWHGSINEGFMMGNPMTKTILHLVHTSELMVAKEF---------
MoNV1-P1 ----AFDDGDDI-EPVEWTGSINEGFMMGNPITKTILHLVHESEHAVATLY---------
Narna-P1
NpNV1-P1 -----PDQAGNY-QLV----SRQRGWMMGDMMTKVILTIAHDAICRMSRLQ---------
WiNV2-P1 -------------QKI-FFCTKLRGWLMGDPMTKVILTLAQEYVLFRSNAG--------R
ScNV20S-P1 -------DGSEI--------TTRRGILMGLPTTWAILNLMHLWCWDSADRQYRLEGHPFR

FIG S2

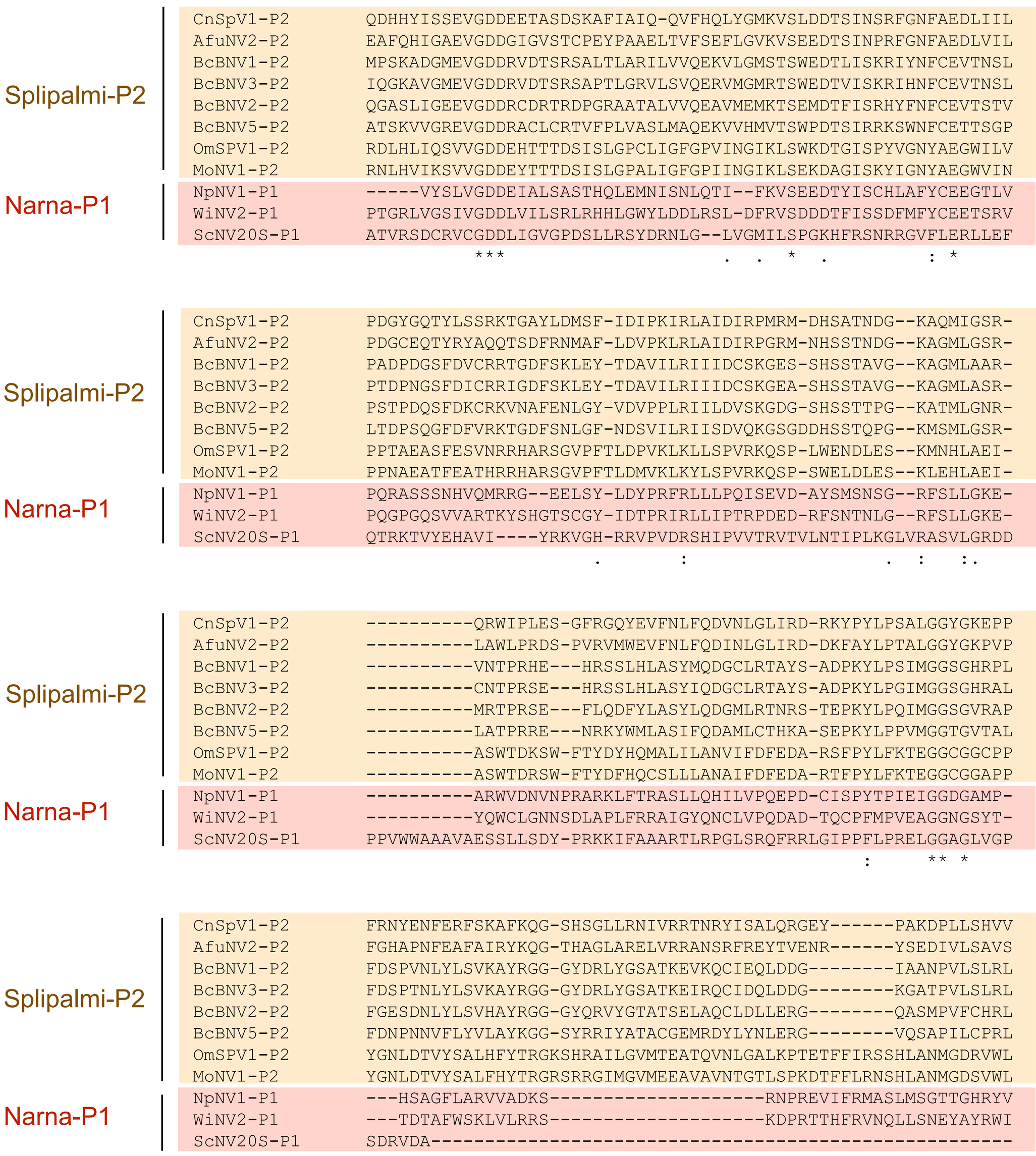
Motif C
Motif D
Splipalmi-P2
CnSpV1-P2 QDHHYISSEVGDDEETASDSKAFIAIQ-QVFHQLYGMKVSLDDTSINSRFGNFAEDLIIL
AfuNV2-P2 EAFQHIGAEVGDDGIGVSTCPEYPAAELTVFSEFLGVKVSEEDTSINPRFGNFAEDLVIL
BcBNV1-P2 MPSKADGMEVGDDRVDTSRSALTLARILVVQEKVLGMSTSWEDTLISKRIYNFCEVTNSL
BcBNV3-P2 IQGKAVGMEVGDDRVDTSRSAPTLGRVLSVQERVMGMRTSWEDTVISKRIHNFCEVTNSL
BcBNV2-P2 QGASLIGEEVGDDRCDRTRDPGRAATALVVQEAVMEMKTSEMDTFISRHYFNFCEVTSTV
BcBNV5-P2 ATSKVVGREVGDDRACLCRTVFPLVASLMAQEKVVHMVTSWPDTSIRRKSWNFCETTSGP
OmSPV1-P2 RDLHLIQSVVGDDEHTTTDSISLGPCLIGFGPVINGIKLSWKDTGISPYVGNYAEGWILV
MoNV1-P2 RNLHVIKSVVGDDEYTTTDSISLGPALIGFGPIINGIKLSEKDAGISKYIGNYAEGWVIN
Narna-P1
NpNV1-P1 -----VYSLVGDDEIALSASTHQLEMNISNLQTI--FKVSEEDTYISCHLAFYCEEGTLV
WiNV2-P1 PTGRLVGSIVGDDLVILSRLRHHLGWYLDDLRSL-DFRVSDDDTFISSDFMFYCEETSRV
ScNV20S-P1 ATVRSDCRVCGDDLIGVGPDSLLRSYDRNLG--LVGMILSPGKHFRSNRRGVFLERLLEF
Splipalmi-P2
CnSpV1-P2 PDGYGQTYLSSRKTGAYLDMSF-IDIPKIRLAIDIRPMRM-DHSATNDG--KAQMIGSR-
AfuNV2-P2 PDGCEQTYRYAQQTSDFRNMAF-LDVPKLRLAIDIRPGRM-NHSSTNDG--KAGMLGSR-
BcBNV1-P2 PADPDGSFDVCRRTGDFSKLEY-TDAVILRIIIDCSKGES-SHSSTAVG--KAGMLAAR-
BcBNV3-P2 PTDPNGSFDICRRIGDFSKLEY-TDAVILRIIIDCSKGEA-SHSSTAVG--KAGMLASR-
BcBNV2-P2 PSTPDQSFDKCRKVNAFENLGY-VDVPPLRIILDVSKGDG-SHSSTTPG--KATMLGNR-
BcBNV5-P2 LTDPSQGFDFVRKTGDFSNLGF-NDSVILRIISDVQKGSGDDHSSTQPG--KMSMLGSR-
OmSPV1-P2 PPTAEASFESVNRRHARSGVPFTLDPVKLKLLSPVRKQSP-LWENDLES--KMNHLAEI-
MoNV1-P2 PPNAEATFEATHRRHARSGVPFTLDMVKLKYLSPVRKQSP-SWELDLES--KLEHLAEI-
Narna-P1
NpNV1-P1 PQRASSSNHVQMRRG--EELSY-LDYPRFRLLLPQISEVD-AYSMSNSG--RFSLLGKE-
WiNV2-P1 PQGPGQSVVARTKYSHGTSCGY-IDTPRIRLLIPTRPDED-RFSNTNLG--RFSLLGKE-
ScNV20S-P1 QTRKTVYEHAVI----YRKVGH-RRVPVDRSHIPVVTRVTVLNTIPLKGLVRASVLGRDD
Splipalmi-P2
CnSpV1-P2 ----------QRWIPLES-GFRGQYEVFNLFQDVNLGLIRD-RKYPYLPSALGGYGKEPP
AfuNV2-P2 ----------LAWLPRDS-PVRVMWEVFNLFQDINLGLIRD-DKFAYLPTALGGYGKPVP
BcBNV1-P2 ----------VNTPRHE---HRSSLHLASYMQDGCLRTAYS-ADPKYLPSIMGGSGHRPL
BcBNV3-P2 ----------CNTPRSE---HRSSLHLASYIQDGCLRTAYS-ADPKYLPGIMGGSGHRAL
BcBNV2-P2 ----------MRTPRSE---FLQDFYLASYLQDGMLRTNRS-TEPKYLPQIMGGSGVRAP
BcBNV5-P2 ----------LATPRRE---NRKYWMLASIFQDAMLCTHKA-SEPKYLPPVMGGTGVTAL
OmSPV1-P2 ----------ASWTDKSW-FTYDYHQMALILANVIFDFEDA-RSFPYLFKTEGGCGGCPP
MoNV1-P2 ----------ASWTDRSW-FTYDFHQCSLLLANAIFDFEDA-RTFPYLFKTEGGCGGAPP
Narna-P1
NpNV1-P1 ----------ARWVDNVNPRARKLFTRASLLQHILVPQEPD-CISPYTPIEIGGDGAMP-
WiNV2-P1 ----------YQWCLGNNSDLAPLFRRAIGYQNCLVPQDAD-TQCPFMPVEAGGNGSYT-
ScNV20S-P1 PPVWWAAAVAESSLLSDY-PRKKIFAAARTLRPGLSRQFRRLGIPPFLPRELGGAGLVGP
Splipalmi-P2
CnSpV1-P2 FRNYENFERFSKAFKQG-SHSGLLRNIVRRTNRYISALQRGEY------PAKDPLLSHVV
AfuNV2-P2 FGHAPNFEAFAIRYKQG-THAGLARELVRRANSRFREYTVENR------YSEDIVLSAVS
BcBNV1-P2 FDSPVNLYLSVKAYRGG-GYDRLYGSATKEVKQCIEQLDDG--------IAANPVLSLRL
BcBNV3-P2 FDSPTNLYLSVKAYRGG-GYDRLYGSATKEIRQCIDQLDDG--------KGATPVLSLRL
BcBNV2-P2 FGESDNLYLSVHAYRGG-GYQRVYGTATSELAQCLDLLERG--------QASMPVFCHRL
BcBNV5-P2 FDNPNNVFLYVLAYKGG-SYRRIYATACGEMRDYLYNLERG--------VQSAPILCPRL
OmSPV1-P2 YGNLDTVYSALHFYTRGKSHRAILGVMTEATQVNLGALKPTETFFIRSSHLANMGDRVWL
MoNV1-P2 YGNLDTVYSALFHYTRGRSRRGIMGVMEEAVAVNTGTLSPKDTFFLRNSHLANMGDSVWL
Narna-P1
NpNV1-P1 ---HSAGFLARVVADKS--------------------RNPREVIFRMASLMSGTTGHRYV
WiNV2-P1 ---TDTAFWSKLVLRRS--------------------KDPRTTHFRVNQLLSNEYAYRWI
ScNV20S-P1 SDRVDA----------

FIG S3

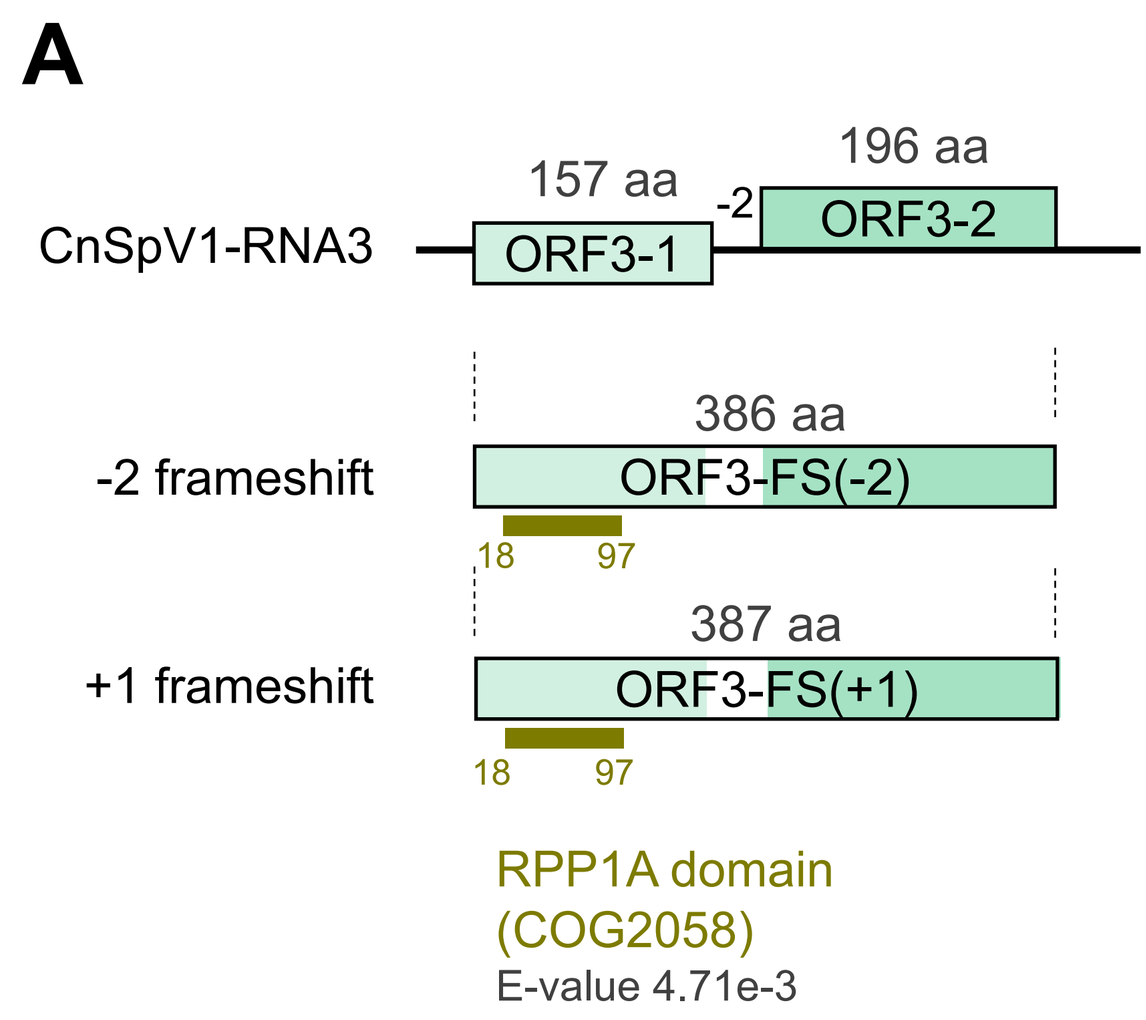
A
157 aa
196 aa
-2
CnSpV1-RNA3
ORF3-1
ORF3-2
386 aa
-2 frameshift
ORF3-FS(-2)
18
97
387 aa
+1 frameshift
ORF3-FS(+1)
18
97
RPP1A domain
(COG2058)
E-value 4.71e-3

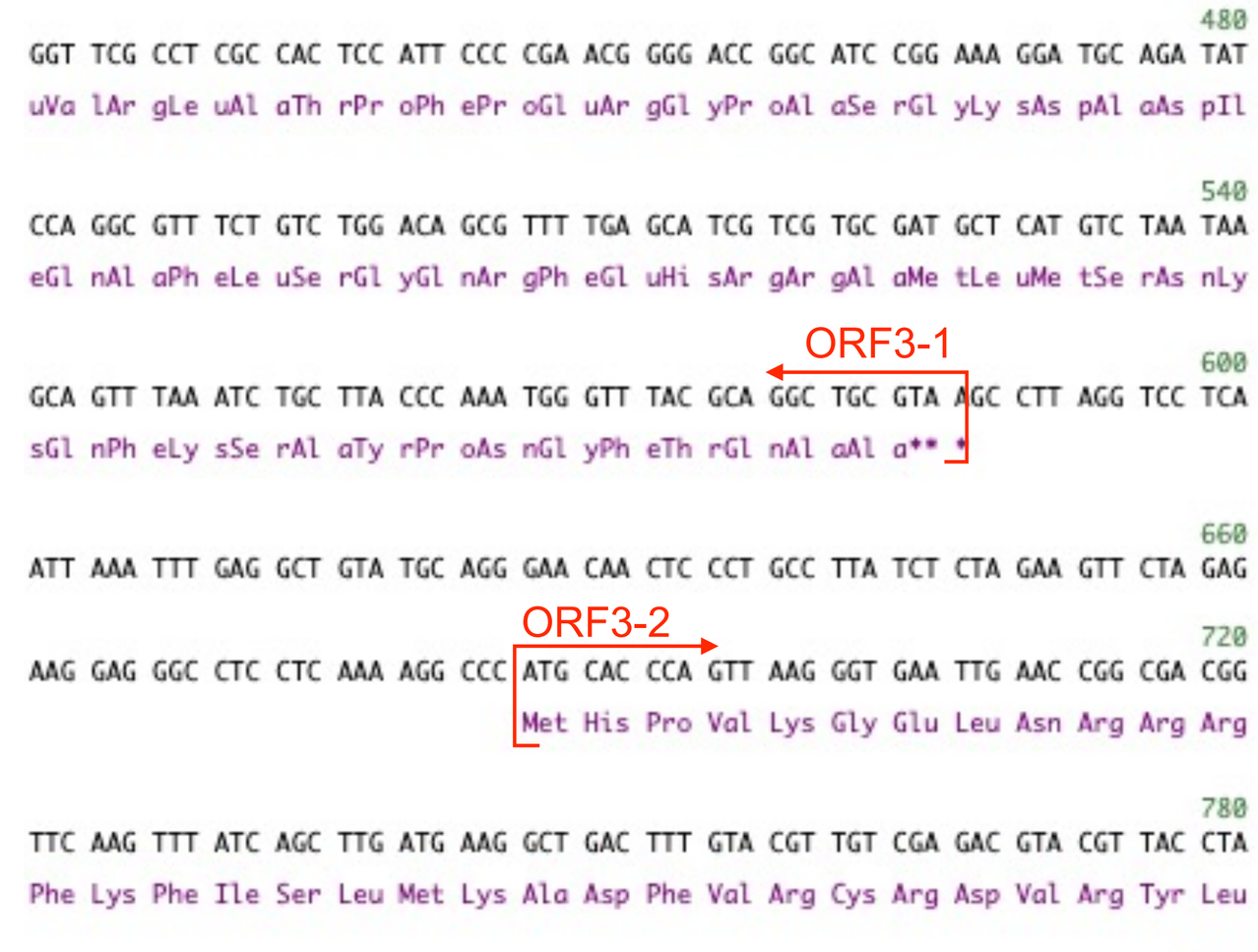
B
480
GGT TCG CCT CGC CAC TCC ATT CCC CGA ACG GGG ACC GGC ATC CGG AAA GGA TGC AGA TAT
uVa lAr gLe uAl aTh rPr oPh ePr oGl uAr gGl yPr oAl aSe rGl yLy sAs pAl aAs pIl
540
CCA GGC GTT TCT GTC TGG ACA GCG TTT TGA GCA TCG TCG TGC GAT GCT CAT GTC TAA TAA
eGl nAl aPh eLe uSe rGl yGl nAr gPh eGl uHi sAr gAr gAl aMe tLe uMe tSe rAs nLy
ORF3-1
600
GCA GTT TAA ATC TGC TTA CCC AAA TGG GTT TAC GCA GGC TGC GTA AGC CTT AGG TCC TCA
sGl nPh eLy sSe rAl aTy rPr oAs nGl yPh eTh rGl nAl aAl a** *
660
ATT AAA TTT GAG GCT GTA TGC AGG GAA CAA CTC CCT GCC TTA TCT CTA GAA GTT CTA GAG
ORF3-2
720
AAG GAG GGC CTC CTC AAA AGG CCC ATG CAC CCA GTT AAG GGT GAA TTG AAC CGG CGA CGG
Met His Pro Val Lys Gly Glu Leu Asn Arg Arg Arg
780
TTC AAG TTT ATC AGC TTG ATG AAG GCT GAC TTT GTA CGT TGT CGA GAC GTA CGT TAC CTA
Phe Lys Phe Ile Ser Leu Met Lys Ala Asp Phe Val Arg Cys Arg Asp Val Arg Tyr Leu

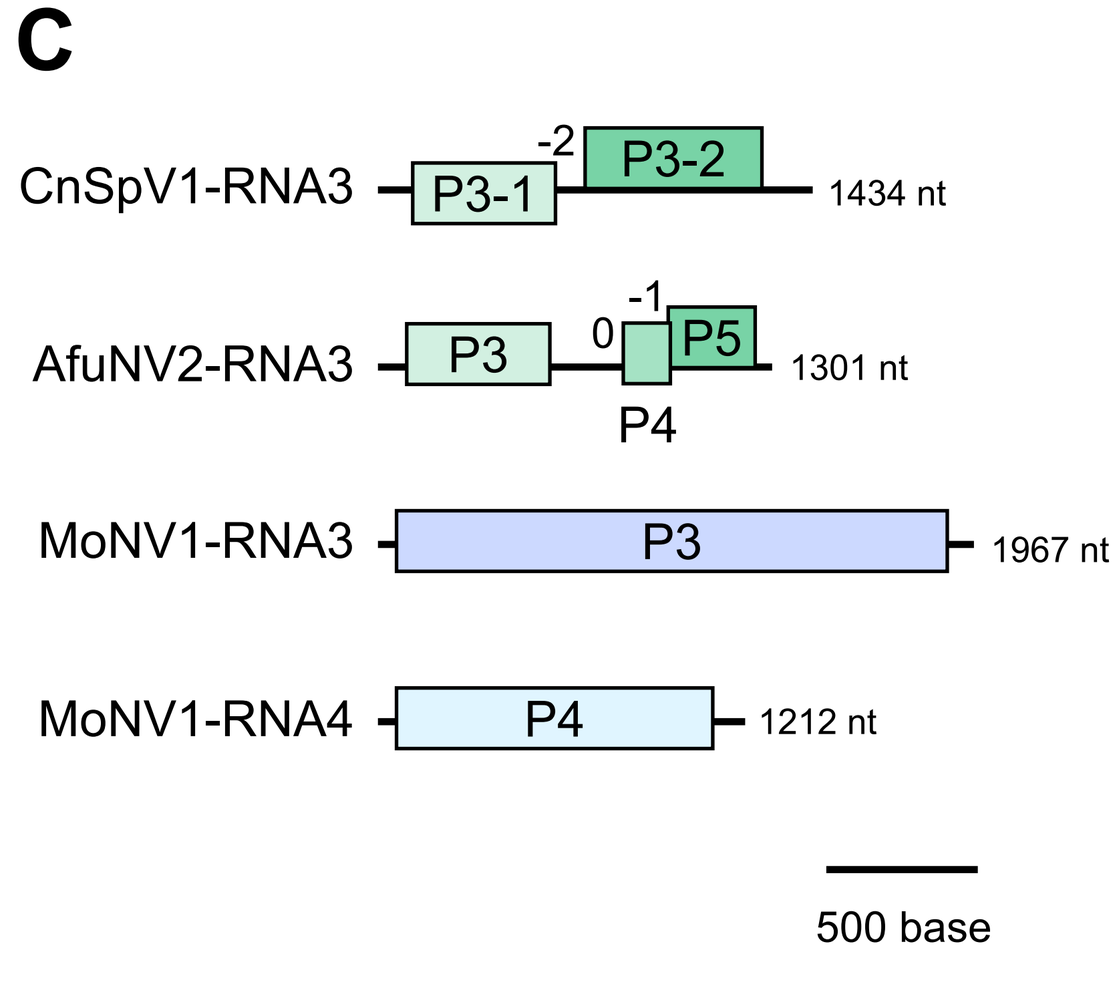
C
CnSpV1-RNA3
-2
P3-1
P3-2
1434 nt
AfuNV2-RNA3
-1
0
P3
P5
P4
1301 nt
MoNV1-RNA3
P3
1967 nt
MoNV1-RNA4
P4
1212 nt
500 base

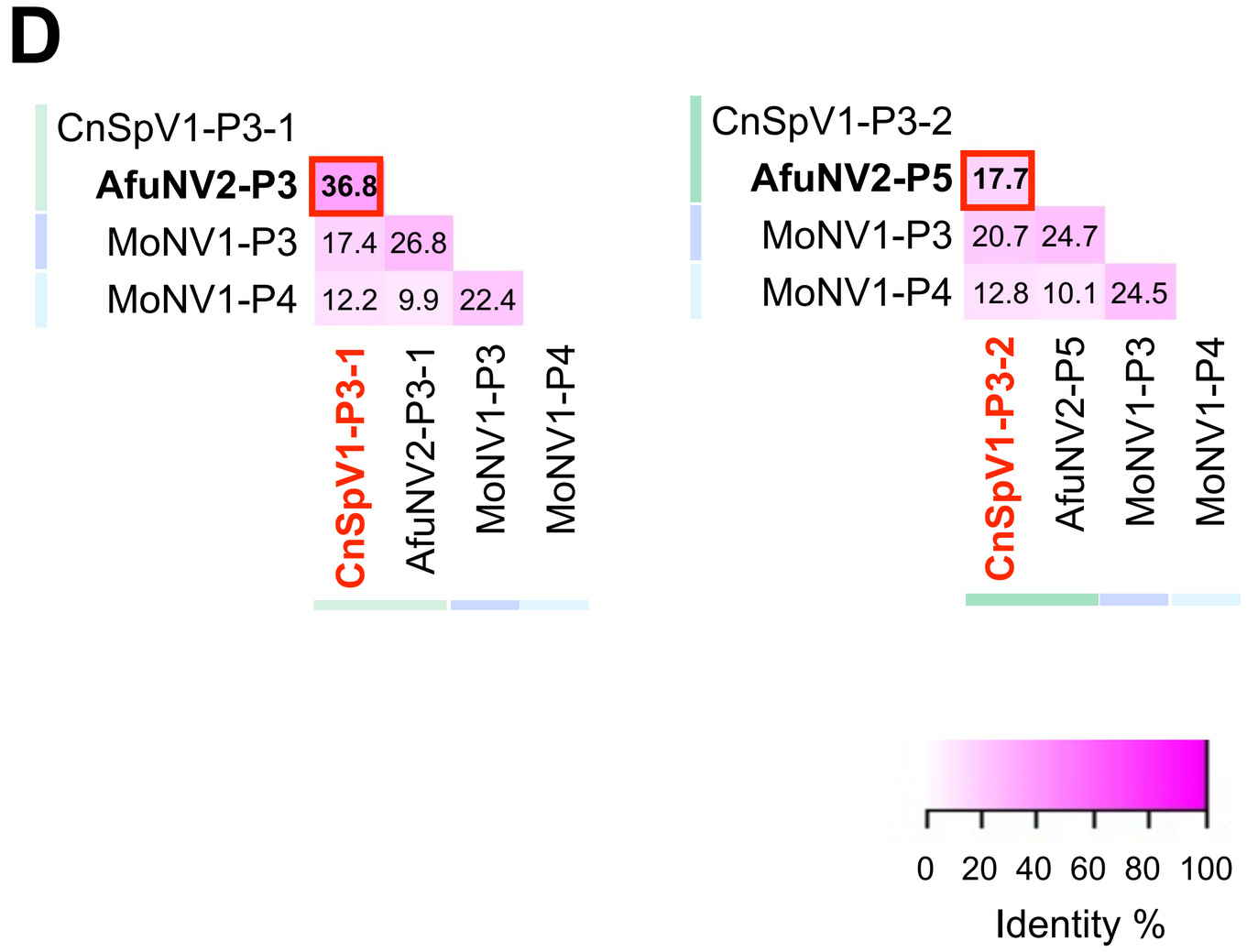
D
CnSpV1-P3-1
AfuNV2-P3 36.8
MoNV1-P3 17.4 26.8
MoNV1-P4 12.2 9.9 22.4
CnSpV1-P3-1
AfuNV2-P3-1
MoNV1-P3
MoNV1-P4
CnSpV1-P3-2
AfuNV2-P5 17.7
MoNV1-P3 20.7 24.7
MoNV1-P4 12.8 10.1 24.5
CnSpV1-P3-2
AfuNV2-P5
MoNV1-P3
MoNV1-P4
0 20 40 60 80 100
Identity %

Table S1. Primers used in this study

For	Target	Primer name	Sequence (5'→3')
RACE	CnSpV1-RNA1-5' terminal	1325-RACE-R	GGGATTGTTTGGTGGGTACCT
	CnSpV1-RNA1-3' terminal	1325-RACE-F	AACCAAGGTCATCCTTCACTA
	CnSpV1-RNA2-5' terminal	700-RACE-R	GATGACATCGTAGGAATTTCA
	CnSpV1-RNA2-3' terminal	700-RACE-F	AACGGTCAGAGTCTACAATAA
	CnSpV1-RNA3-5' terminal	Narna1142-700F	TCAAAAGGCCCATGCACCCAG
	CnSpV1-RNA3-3' terminal	Narna1142-730R	TCACCCTTAACTGGGTGCATG
	CnSpV1-RNA4-5' terminal	CnSpV1-RNA4-638R	ACCTTTGGTATGCTTTACCA
	CnSpV1-RNA4-3' terminal	CnSpV1-RNA4-190F	CAAGGAGAACTGTGAAGTTC
RT-PCR, DIG labelling PCR	CnSpV1-RNA1 (1301-2000 nt)	EU-Cp1325-1300F	GCGGGAAGCTTGAACGCGCCC
		EU-Cp1325-2000R	AGTGCCATCACAGCACTCTCT
	CnSpV1-RNA2 (317-826 nt)	EU-Cp700-300F	TAAAATCCTTCAATCTTATGG
		EU-Cp700-800R	GCACTGGGTAAATAGGGATAT
	CnSpV1-RNA3 (204-704 nt)	Narna1142-230F	AGTATCAGAAGATGCTTGGTAAAG
		Narna1142-730R	*See above*
	CnSpV1-RNA4 (190-638 nt)	CnSpV1-RNA4-190F	*See above*
		CnSpV1-RNA4-638R	*See above*
	CnFGV1 (5625-6650 nt)	FGRdF	TTCACAACTAAAGCATCTGAGCGG
		FGRdR	CGATGGGTATGATTGCCTGCC

Table S2. Accession numbers for splipalmiviral proteins

Classification	Virus name	Virus abbrev.	P1	P2	P3	P4	P5
Splipalmivirus	Aspergillus fumigatus narnavirus 2	AfuNV2	BCH36622.1	BCH36623.1	BCH36624.1	-	BCH36625.1
	Botrytis cinerea binarnavirus 1	BcBNV1	QJT73724.1	QTP72364.1	-	-	-
	Botrytis cinerea binarnavirus 2	BcBNV2	QJT73725.1	QLF49184.1	-	-	-
	Botrytis cinerea binarnavirus 3	BcBNV3	QJT73726.1	QTP72363.1	-	-	-
	Botrytis cinerea binarnavirus 5	BcBNV5	QJT73728.1	QTP72365.1	-	-	-
	Oidiodendron maius splipalmivirus 1	OmSPV1	QNN89179.1	QNN89180.1	-	-	-
	Magnaporthe oryzae narnavirus 1	MoNV1	BCH36656.1	BCH36655.1	BCH36657.1	BCH36658.1	-
Narnavirus	Neofusicoccum parvum narnavirus 1	NpNV1	QDB74994.1	-	-	-	-
	Wilkie narna-like virus 2	WiNV2	YP_009388579.1	-	-	-	-
	Saccharomyces 20S RNA narnavirus	ScNV20S	NP_660178.1	-	-	-	-

64 **Table S3. Local-blastn analyses with the obtained contig sequences.**

Name	Consensus length	Total read count	Average coverage	Lowest E-value	Accession	Description
Crypho_mix_contig_41_mapping	9799	72351	736.8148	3.18E-34	NC_030202	Fusarium poae dsRNA virus 3 isolate SX63, complete genome
Crypho_mix_contig_43_mapping	8747	51776	590.7544	1.79E-11	NC_040828	Trichoderma asperellum dsRNA virus 1 isolate JLM45-3 hypothetical protein and RdRP genes, complete cds
Crypho_mix_contig_91_mapping	8827	15163	171.2978	1.14E-07	NC_040828	Trichoderma asperellum dsRNA virus 1 isolate JLM45-3 hypothetical protein and RdRP genes, complete cds
Crypho_mix_contig_700_mapping*	2264	1371	60.50751	1.55E-07	NC_035120	Wilkie narna-like virus 2 strain mosWSCP85442, complete genome
Crypho_mix_contig_1325_mapping	2144	751	34.90065	6.02E-61	NC_030866	Fusarium poae narnavirus 2 genomic RNA, complete genome
Crypho_mix_contig_152_mapping	765	20178	2614.765	0	NC_001492	Cryphonectria hypovirus 1, complete genome
Crypho_mix_contig_151_mapping	354	4639	1279.768	1.67E-96	NC_001492	Cryphonectria hypovirus 1, complete genome
Crypho_mix_contig_150_mapping	354	3073	843.2514	1.67E-96	NC_001492	Cryphonectria hypovirus 1, complete genome
Crypho_mix_contig_34_mapping	3120	68082	2138.204	0	NC_001492	Cryphonectria hypovirus 1, complete genome
Crypho_mix_contig_45_mapping	6750	145949	2162.524	0	NC_001492	Cryphonectria hypovirus 1, complete genome
Crypho_mix_contig_46_mapping	6814	92206	1352.551	0	NC_001492	Cryphonectria hypovirus 1, complete genome
Crypho_mix_contig_651_mapping	3285	7484	227.4755	0	NC_038781	Cryphonectria nitschkei chrysovirus 1 strain BS122 putative cysteine protease gene, complete cds
Crypho_mix_contig_219_mapping	3130	6815	217.3629	0	NC_038780	Cryphonectria nitschkei chrysovirus 1 strain BS122 putative replication associated protein gene, complete cds
Crypho_mix_contig_835_mapping	3107	5874	189.0148	0	NC_038779	Cryphonectria nitschkei chrysovirus 1 from Cryphonectria nitschkei BS122 capsid protein gene, complete cds
Crypho_mix_contig_192_mapping	3428	5333	155.4758	0	NC_038778	Cryphonectria nitschkei chrysovirus 1 from Cryphonectria nitschkei BS122 RdRP, complete cds
Crypho_mix_contig_128_mapping	346	2745	784.2254	6.1E-159	NC_021222	Cryphonectria parasitica bipartite mycovirus 1 strain 09269 segment RNA1, complete sequence
Crypho_mix_contig_1015_mapping	387	2861	737.3204	1E-175	NC_021222	Cryphonectria parasitica bipartite mycovirus 1 strain 09269 segment RNA1, complete sequence
Crypho_mix_contig_129_mapping	1703	9853	575.3235	0	NC_021222	Cryphonectria parasitica bipartite mycovirus 1 strain 09269 segment RNA1, complete sequence
Crypho_mix_contig_185_mapping	832	4415	530.0505	0	NC_021222	Cryphonectria parasitica bipartite mycovirus 1 strain 09269 segment RNA1, complete sequence

Crypho_mix_contig_179_mapping	310	1359	433.7226	1.2E-116	NC_021222	Cryphonectria parasitica bipartite mycovirus 1 strain 09269 segment RNA1, complete sequence
Crypho_mix_contig_139_mapping	791	2724	344.2389	0	NC_021222	Cryphonectria parasitica bipartite mycovirus 1 strain 09269 segment RNA1, complete sequence
Crypho_mix_contig_1997_mapping	311	542	170.1897	1.7E-127	NC_021222	Cryphonectria parasitica bipartite mycovirus 1 strain 09269 segment RNA1, com+A20:G21plete sequence
Crypho_mix_contig_833_mapping	537	2318	428.5736	0	NC_021223	Cryphonectria parasitica bipartite mycovirus 1 strain 09269 segment RNA2, complete sequence
Crypho_mix_contig_72_mapping	989	4123	412.8878	0	NC_021223	Cryphonectria parasitica bipartite mycovirus 1 strain 09269 segment RNA2, complete sequence
Crypho_mix_contig_71_mapping	1049	3288	288.5844	0	NC_021223	Cryphonectria parasitica bipartite mycovirus 1 strain 09269 segment RNA2, complete sequence
Crypho_mix_contig_108_mapping	1651	4748	286.1896	0	NC_021223	Cryphonectria parasitica bipartite mycovirus 1 strain 09269 segment RNA2, complete sequence
Crypho_mix_contig_948_mapping	536	1436	266.916	0	NC_021223	Cryphonectria parasitica bipartite mycovirus 1 strain 09269 segment RNA2, complete sequence

* The result of blastp search is shown for this contig.